MODELING THE LONG-TERM FLUVIAL REDISTRIBUTION OF TEPHRA IN FORTYMILE WASH, YUCCA MOUNTAIN, NEVADA

Prepared for

U.S. Nuclear Regulatory Commission
Contract NRC–02–02–012

Prepared by

Donald M. Hooper

Center for Nuclear Waste Regulatory Analyses
San Antonio, Texas

July 2005

ABSTRACT

A sediment budget approach has been formulated to model the long-term fluvial redistribution of basaltic tephra in Fortymile Wash at Yucca Mountain, Nevada. In the event of a volcanic eruption through the potential repository, high-level waste also may be transported in the volcanic tephra plume, with the potential deposition of radionuclides at the reasonably maximally exposed individual (or receptor) location either from direct sedimentation from the volcanic ash cloud or from the remobilization of tephra by water and wind after initial deposition.

Fortymile Wash is an ephemeral stream; hydrologic data are minimal, and sediment transport data are lacking. Rates of erosion in arid regions are not well-constrained, but a suitable range of values can be entered into a sediment budget to demonstrate the quantitative or mass flux relationship between such components as sediment yield, discharge to the depositional fan, balance of remaining tephra, dilution by mixing with ambient sediment, and associated changes in transient sediment storage. Using parameters specific to Fortymile Wash and a potential tephra-forming eruption at Yucca Mountain, the redistribution model shows that substantial tephra deposits can persist for over 1,000 years in arid terrains, even with a period of accelerated erosion immediately following the eruption. For example, in a scenario employing statistical means for key parameters, approximately 98 percent of the tephra deposit remains in the Fortymile Wash catchment basin after 100 years and 50 percent of the tephra deposit remains after 1,800 years. Therefore, the model shows that the amount of remobilized tephra may be large—even when mixed with ambient sediment—and could significantly affect airborne particle concentrations for the reasonably maximally exposed individual. Posteruption remobilization of tephra appears potentially risk significant as redistributed tephra deposits may sustain airborne mass loads and associated inhalation doses for longer periods of time than indicated by simple decay relationships for the original volcanic deposits.

This report communicates the current understanding of tephra redistribution analyses independently developed by Center for Nuclear Waste Regulatory Analyses (CNWRA) staff. The results of these volcanological and geomorphological investigations are being used to refine model parameters for performance assessment calculations, to refine risk insights, and to support staff review of the potential U.S. Department of Energy (DOE) license application for a high-level waste repository at Yucca Mountain.

CONTENTS

CONTENTS (continued)

FIGURES

TABLES

ACKNOWLEDGMENTS

This report was prepared to document work performed by the Center for Nuclear Waste Regulatory Analyses (CNWRA) for the U.S. Nuclear Regulatory Commission (NRC) under Contract No. NRC–02–02–012. The activities reported here were performed on behalf of the NRC Office of Nuclear Material Safety and Safeguards, Division of High-Level Waste Repository Safety. The report is an independent product of CNWRA and does not necessarily reflect the views or regulatory position of NRC.

This report was improved by reviews from Brittain E. Hill and Sitakanta Mohanty. The author is grateful to Sharon Odam and Ruth Mantooth for assisting with the word processing and preparation of the final report. D. Marius Necsoiu, Deborah Waiting, and Brittain E. Hill provided aid with figure production and Erika Hanson conducted the editorial review. The author wishes to thank Brittain Hill, Roland Benke, John Trapp (NRC), James Rubenstone (NRC), Keith Compton (NRC), Richard Codell (NRC), Razvan Nes, Sitakanta Mohanty, D. Marius Necsoiu, H. Lawrence McKague, John Stamatakos, and Brandi Winfrey for thoughtful discussions and support during the course of this work.

QUALITY OF DATA, ANALYSES, AND CODE DEVELOPMENT

DATA: All CNWRA-generated original data contained within this report were collected and analyzed to meet quality assurance requirements as described in the CNWRA Quality Assurance Manual. Sources for all other data should be consulted to determine the level of quality of these data.

ANALYSES AND CODES: Calculations were checked as required by QAP–014, Documentation and Verification of Scientific and Engineering Calculations and recorded in a scientific notebook. Commercially-available software KaleidaGraph® Version 3.0 and Microsoft® Excel were used for spreadsheets and plotting of data. Generation of figures was aided by the use of Adobe® Photoshop Version 7.0.1, ArcGIS 8.3, Arc/Info 7.0.2, ArcView 3.2, and Adobe Illustrator Version 10.0.3.

1 INTRODUCTION

1.1 Background

Yucca Mountain, Nye County, Nevada, has been identified as a potential site for the underground disposal of high-level waste. Basaltic igneous activity has occurred for over 10 million years throughout the Yucca Mountain area and has necessitated more than 20 years of volcanic hazard studies by the U.S. Department of Energy (DOE), the U.S. Nuclear Regulatory Commission (NRC), and the State of Nevada. A key component of these studies is quantifying the likelihood that a new basaltic volcano could form at the potential repository site during the postclosure period. Under this scenario there is the potential for volcanic disruption of some waste packages. Waste could be entrained in the subvolcanic conduit and dispersed in the eruption plume, thereby enabling the airborne transport of radionuclides. The volcanic ejecta (a mix of ash, cinders, bombs, and blocks collectively referred to as tephra) would be dispersed according to such factors as height of the eruption column, particle size distribution, and structure of the winds aloft.

Following a potential volcanic eruption, a submillimeter-to-meters thick [1 mm = 0.04 in and 1 m = 3.3 ft.] deposit of tephra could be deposited on hillslopes around Yucca Mountain that are part of the Fortymile Wash drainage basin. Contaminated tephra-fall deposits would be affected by subsequent surface processes and remobilized. The transport of material by wind is eolian remobilization, which may include the resuspension of fine tephra following the initial deposition from a volcanic eruption plume. The transport of material by surficial water processes is referred to as fluvial remobilization, which may include redistribution and sediment mixing of tephra in Fortymile Wash. Tephra would be eroded by mass wasting (including soil creep and shallow landslides), the combined effects of raindrop splash and sheet wash, channel erosion (including rilling and gullying), and eolian processes. In arid areas like Yucca Mountain in southern Nevada, sediment remobilization and redistribution processes are not well understood, and supporting data are sparse. Remobilized tephra is expected to follow a path similar to existing sediments (i.e., down the Fortymile Wash drainage system during periods of episodic overland flow). The quantitative extent of erosion and sediment transport caused by floods in ephemeral Fortymile Wash is unknown (Squires and Young, 1984). In the existing Fortymile Wash system, transported sediments begin to accumulate several kilometers [1 km = 0.62 mi] north of the location of the reasonably maximally exposed individual or receptor. At this location, the main Fortymile Wash drainage changes from a steep-sided incising channel to a broad, braided fan depositional system. Existing sediment deposition continues south into the Amargosa Desert and overlaps the general area of the reasonably maximally exposed individual location near the southern boundary of the Nevada test site. Surface winds can entrain fine-grained particles contaminated by high-level waste from the remobilized deposits, which can then be inhaled by the nearby receptor. The reasonably maximally exposed individual location can be described generally by the uninhabited areas within several kilometers of the Fortymile Wash drainage along the southern boundary of the Nevada test site (Bechtel SAIC Company, LLC., 2003a). This is approximately 18 km [11.2 mi] from the potential repository site in the vicinity of the Fortymile Wash depositional fan.

This report describes a simplified process-level model that has been developed to evaluate the long-term fluvial redistribution of tephra following a scoria-cone (or violent strombolian) eruption. A sediment budget approach is incorporated as a fundamental part of this model to maintain mass balance as erosion, storage, transport, and deposition progresses within the

Fortymile Wash drainage system as a function of time after the eruption. This model attempts to provide a clear methodology to relate geomorphic processes and rates observed approximately over the last 10,000 years in Fortymile Wash to processes and rates likely to occur if appreciable amounts of easily redistributed volcanic tephra are deposited in this drainage system. The sediment budget methodology was first applied to the tephra deposit from the 1943–1952 eruption of Parícutin Volcano, Mexico (Hooper, 2004; Hooper and Hill, 2004), and the present study represents the evolution of that first-order conceptual model. Appropriate model parameters have been substantiated for expected dryland conditions following a modeled eruption at Yucca Mountain. To the greatest extent possible, analyses consider appropriate uncertainties in model data and address site-specific processes. Eolian remobilization is not treated specifically in this model, but will be incorporated as a separate process (Benke, et al., 2005) into the latest version of the Total-system Performance Assessment (TPA) code.

1.2 Risk Significance

In the event of a volcanic eruption through the potential repository, contaminated tephra could be deposited over hundreds to perhaps thousands of square kilometers [tens to perhaps hundreds of square miles]. Over time, some of this tephra can be eroded and transported by water and wind, with later deposition at or near the location of the reasonably maximally exposed individual or receptor. An influx of redistributed tephra could affect the airborne particle concentrations at the receptor location, depending on the rate of remobilization and dilution with existing sediments. Resuspension of fine-grained ash particles produces airborne concentrations (or the airborne mass load) of ash and high-level waste. Inhalation of resuspended volcanic ash or tephra dominates the total dose for the igneous activity scenario. Airborne mass load for the years following a potential volcanic eruption is a high sensitivity parameter in total-system performance assessment calculations (Mohanty, et al., 2005, 2004), and uncertainties in this parameter strongly affect calculations of expected annual dose. For extrusive volcanism, remobilization is directly related to the four risk insights presented in the Risk Insights Baseline Report (NRC, 2004):

- Inhalation of resuspended volcanic ash (high significance to waste isolation)
- Remobilization of ash deposits (medium significance to waste isolation)
- Wind vectors during an eruption (medium significance to waste isolation)
- Volume of ash produced by an eruption (medium significance to waste isolation)

Remobilization and redistribution processes may considerably affect the thickness of a potential tephra deposit near the reasonably maximally exposed individual and the extent of eventual mixing of tephra with underlying soil, which both factor into the proportion of ash in the airborne mass load. Simple mass-balance scoping calculations (Hill and Connor, 2000; Hooper, 2004) and results from the present study indicate that the accumulation rate of fluvially remobilized tephra may exceed the decay rate in airborne particle concentration from the original volcanic deposit at the reasonably maximally exposed individual location. Thus, remobilization of potential tephra deposits may sustain airborne particle concentrations and associated inhalation doses to the reasonably maximally exposed individual for longer periods of time than indicated by simple decay relationships for original volcanic deposits (e.g., Bechtel SAIC Company, LLC., 2004; 2003b,c,d).

The sediment budget approach developed in this report ensures that NRC licensing decisions can be based on realistic volcanological and geomorphological models and data. The DOE model for tephra redistribution does not evaluate geomorphological processes that are likely to affect redistribution of potential tephra deposits in the Fortymile Wash drainage system (Kokajko, 2005). The DOE model is not supported by comparison to detailed process-level models or empirical observations, and tephra dilution rates do not have a clear or traceable analogy to potential tephra deposits in the Fortymile Wash drainage system. Insights gained from this report on the long-term fluvial redistribution of tephra in Fortymile Wash will help staff prepare a technical basis to review DOE models that address remobilization and redistribution.

1.3 Report Content

The remainder of Chapter 1 discusses streamflow characteristics at Yucca Mountain, reviews erosion at Yucca Mountain, reviews analog volcanoes, and describes the sediment budget approach for redistribution modeling. Emplacement of tephra-fall deposits can disrupt sediment routing in watersheds. The geomorphologic response to such a landscape disturbance may be particularly significant and prolonged, resulting in posteruption sediment yields that exceed preeruption yields. The sediment budget concept and model is developed throughout this report to address the linkages between sediment sources, sediment volume, transport processes, and storage.

A flood-frequency analysis is presented in Chapter 2. The flood-frequency curve reflects a large uncertainty in recurrence rate, but this analysis assigns a value of 4 years to the TPA code parameter TimeBetweenFlowEvents[yr]. Tephra dispersal parameters for redistribution and sediment accumulation rates in the Fortymile Wash depositional fan are described in Chapter 3.

Chapter 4 develops an abstracted model that combines empiricism and numerical modeling in order to quantify accelerated erosion and its impact on sediment yield in Fortymile Wash following a potential tephra-fall eruption. Redistribution modeling results are presented in Chapter 5.

1.4 Streamflow Characteristics at Yucca Mountain, Nevada

1.4.1 Background

Fortymile Wash is an ephemeral stream system that drains the rugged, arid terrain of southwestern Nevada. The length of time between streamflow events can be several years, and no perennial streams exist in the area. Runoff is infrequent because of high evapotranspiration rates and a low annual precipitation of approximately 150 mm [6 in] per year. Modern climate summaries for the Yucca Mountain area and western U.S. stations can be found at:

- http://www/yuccamountain.dri.edu
- http://www.wrcc.dri.edu/climsum.html
- http://wwwsord.nv.doe.gov/SORD_Rain.html

Drylands is a collective term for arid, semiarid, and dry subhumid regions such as the Yucca Mountain area. Characteristic properties of drylands include ephemeral stream flow and watersheds supporting sparse, unevenly distributed, or temporally variable vegetation covers. Relevant works by Graf (1988), Tooth (2000), and Bull and Kirkby (2002) specifically discuss fluvial processes in dryland drainage systems.

Ephemeral streams, which tend to have wide channels, have a high ratio of sediment-to-water compared to humid-temperate rivers (Bull and Kirkby, 2002). Because streamflow is so uncommon, any flow may be considered locally to be a flood. When dryland rivers are in flood they are also efficient erosional agents than perennial systems (Laronne and Reid, 1993). However, infiltration losses are high. Sediment transport in dryland rivers tends to be more transport limited than supply limited (Graf, 1988).

Yucca Mountain is a long north-trending ridge with an average ridge-crest altitude of approximately 1,500 m [4,921 ft]. The long ridgeline divides the drainage basins of Crater Flat to the west from Fortymile Wash to the east. Fortymile Wash drains from north to south, and the watershed area is 815 km^2 [315 mi^2]. Ephemeral streams on the east side of Yucca Mountain are tributary to Fortymile Wash, which heads on Pahute Mesa and flows southward through Fortymile Canyon ≈ 40 km [25 mi] before flowing into a broad distributary network (or depositional basin) in the Amargosa Desert near the town of Amargosa Valley, Nevada. During major floods, the distributary system of Fortymile Wash may join the Amargosa River and flow into Death Valley in southeastern California.

Prior to their decommissioning, the streamflow gaging network in the Yucca Mountain area consisted of continuous-record gaging stations, peak flow crest-stage gages, and miscellaneous sites (Kane, et al., 1994; Pabst, et al., 1993; Savard, 1998). Each surface-water data station is assigned a unique identification number (e.g., Pabst, et al., 1993). Downstream order along a stream is represented by the sequential numbering of stations. Gaps are left in the series to allow for new stations; hence, the numbers are not consecutive. For example, the complete 8-digit number for Station 10251258 includes the 2-digit part number 10, plus the 6-digit downstream-order number 251258. Part 10 refers to the Great Basin drainage system. The relevant streamflow gaging stations are described in Table 1-1.

The Fortymile Wash drainage basin can be divided into four sections or reaches, from north to south (Figure 1-1):

(1) Fortymile Canyon reach or the upper headwater area: upstream from Fortymile Wash at the Narrows (Station 10251250) to the Pah Canyon confluence, a distance of 7.1 km [4.4 mi]

(2) Upper Jackass Flats reach: the incised channel from the Narrows to near Well J–13 (Station 10251255), a distance of 10.1 km [6.3 mi]

(3) Lower Jackass Flats reach: the incised channel from near Well J–13 to Fortymile Wash near the settlement of Amargosa Valley (Station 10251258), a distance of 16.8 km [10.4 mi]

(4) Amargosa Desert reach: downstream from Fortymile Wash near the town of Amargosa Valley as part of a broad distributary network

Table 1-1. Selected Surface Water Data Collection Sites in the Fortymile Wash Drainage Basin near Yucca Mountain, Nevada				
Station Number*	**Station Name**	**Latitude and Longitude**	**Drainage Area (km^2)**	**Site Type† and Period of Record**
10251250	Fortymile Wash at Narrows, Nevada Test Site	36° 53' 13" 116° 22' 50"	668	C: 1982–1983 G: September 21, 1983–1997
10251252	Yucca Mountain Wash near Mouth (Tributary), Nevada Test Site	36° 51' 58" 116° 23' 38"	44.0	C: 1982–1995
10251254	Drillhole Wash at Mouth (Tributary), Nevada Test Site	36° 49' 13" 116° 23' 52"	42.2	C: 1983–1995
10251255	Fortymile Wash near Well J-13, Nevada Test Site	36° 48' 27" 116° 24' 01"	787	M: 1969 and 1983 G: November 30, 1983–1997
10251256	Dune Wash near Busted Butte (tributary), Nevada Test Site	36° 47' 35" 116° 24' 29"	17.5	C: 1982–1995
10251258	Fortymile Wash near Amargosa Valley, Nevada	36° 40' 18" 116° 26' 03"	815.3‡	M: 1969 C: 1982–1983 G: November 15, 1983–1997

Sources: Pabst, et al., 1993; Savard, 1998; CRWMS M&O, 2000.

*Station numbers are assigned in downstream order from uppermost location.
†C = crest-stage gage; G = continuous gaging station; M = miscellaneous site.
‡U.S. Geological Survey publications use a drainage area of 818 km^2 [316 mi^2] [1 km^2 = 0.386 mi^2].

1.4.2 Fortymile Wash Streamflow, 1969–1998

Streamflow data were collected from 1969 to 1998 by the U.S. Geological Survey following standard methods and procedures in various U.S. Geological Survey publications. Details regarding individual streamflow events can be found in Beck and Glancy (1995); Kane, et al. (1994); Pabst, et al. (1993); Tanko and Glancy (2001); and Waddell, et al. (1984). There were no large-volume, gage-to-gage streamflow measured in Fortymile Wash from 1970 through 1982. Peak discharge measurements at stream gaging sites in the Fortymile Wash area are summarized in Table 1-2.

Squires and Young (1984) examined the flood potential of Fortymile Wash and its principal southwestern tributaries. Savard (1998) estimated groundwater recharge from streamflow and calculated infiltration loss associated with the Fortymile Wash drainage system (Table 1-3). Streamflow infiltration loss volumes for each reach were estimated using a streamflow volume

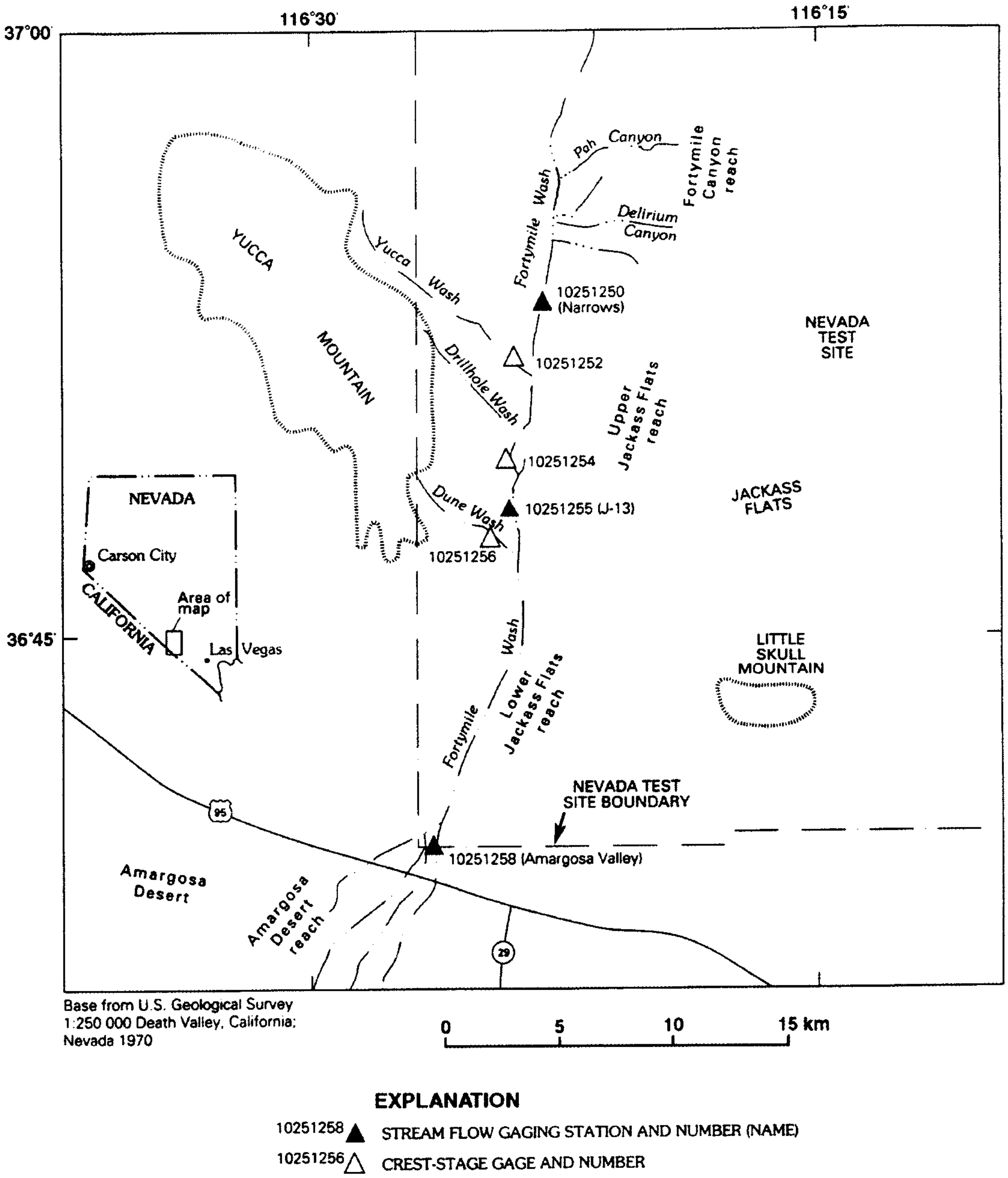

Figure 1-1. Location of Streamflow Gaging Stations and Crest-Stage Gages in the Fortymile Wash Drainage Basin Near Yucca Mountain, Nevada (Modified from Savard, 1998).

Table 1-2. Peak Discharges at Stream Gaging Sites in the Fortymile Wash Area						
Date	Peak Discharge (m^3/s) [1 m^3/s = 35.3 ft^3/s]					
	10251250 Fortymile Wash at Narrows	10251252 Yucca Wash Near Mouth (Tributary)	10251254 Drillhole Wash at Mouth (Tributary)	10251255 Fortymile Wash Near Well J–13	10251256 Dune Wash Near Busted Butte (Tributary)	10251258 Fortymile Wash Near Amargosa Valley
January 25, 1969	—*	—	—	—	—	42.5
February 24–26, 1969	—	—	—	570	—	93.5
March 3, 1983	43.0	2.83	—	16.1	—	11.3
July 21–23, 1984	20.7	26.6	22.4	52.7	—	40.5
August 14–16, 1984	1.42	—	—	—	—	—
August 18–20, 1984	19.3	0.88	1.22	24.4	0.40	10.5
July 19–20, 1985	0.33	0.0003	0.48	0.17	2.66	0.09
February 23, 1987	—	—	—	—	—	0.02
May 7, 1987	—	< 0.003	—	—	—	—
November 6, 1987	—	—	—	—	—	0.02
September 23, 1990	—	—	—	—	—	0.02
August 12–13, 1991	—	—	—	—	—	—
September 7, 1991	—	—	—	—	0.12	—
February 12–15, 1992	0.68	0.42	—	—	0.04	—
March 30–31, 1992	—	< 0.03	—	—	0.03	—

Table 1-2. Peak Discharges at Stream Gaging Sites in the Fortymile Wash Area (continued)

Date	Peak Discharge (m^3/s) [1 m^3/s = 35.3 ft^3/s]					
	10251250 Fortymile Wash at Narrows	10251252 Yucca Wash Near Mouth (Tributary)	10251254 Drillhole Wash at Mouth (Tributary)	10251255 Fortymile Wash Near Well J-13	10251256 Dune Wash Near Busted Butte (Tributary)	10251258 Fortymile Wash Near Amargosa Valley
January 17–19, 1993	1.50	2.26	—	—	—	—
February 9, 1993	—	—	—	—	—	—
February 23, 1993	—	—	—	—	—	—
January 25–27, 1995	0.20	5.24	—	—	0.08	—
March 11–13, 1995	85.0	—	0.003	85.0	0.08	34.0
February 23–24, 1998†	5.7	6.2	0.7	5.7	nd‡	9.6

Sources: CRWMS M&O, 2000; Tanko and Glancy, 2001

*Dash symbol means either no streamflow was recorded or stream gaging site was not operating during period of streamflow.
†Cumulative streamflow volumes for the 1995 and 1998 storm runoffs were estimated differently because most of the streamflow gaging stations were discontinued prior to the 1998 flood.
‡Site disturbed by road crews prior to measurements (nd = not determined).

Table 1-3. Measured and Estimated Volumes (in Cubic Meters) of Streamflow and Infiltration Losses for the Four Reaches of Fortymile Wash

Volume (m^3) [1 m^3 = 35.3 ft^3]									
Date	Estimated Fortymile Canyon Infiltration Loss*	Measured Narrows Gage (10251250)	Estimated Upper Jackass Flats Tributary Inflow	Estimated Upper Jackass Flats Infiltration Loss	Measured J-13 Gage (10251255)	Estimated Lower Jackass Flats Tributary Inflow	Estimated Lower Jackass Flats Infiltration Loss	Measured Amargosa Valley Gage (10251258)	Estimated Amargosa Desert Infiltration Loss
Jan. 25, 1969	**51,800**	—	—	**73,700**	—	—	**123,000**	—	**280,000**
Feb. 24–26, 1969	**51,800**	—	—	**73,700**	—	—	**123,000**	—	**440,000**
March 3, 1983	**51,800**	—	—	**73,700**	—	—	**123,000**	—	**128,000**
July 21–23, 1984	**51,800**	162,000	108,000	**73,700**	196,000	0	**123,000**	273,000	**273,000**
Aug. 14–16, 1984	**51,800**	10,500	—	**10,500**	3,600	—	**3,600**	1,200	**1,200**
Aug. 18–20, 1984	**51,800**	140,000	51,700	**73,700**	118,000	133,000	**123,000**	128,000	**128,000**
July 19–20, 1985	**4,800**	980	8,130	**8,280**	830	22,140	**22,730**	240	**240**
Feb. 23, 1987	**0**	0	0	**0**	0	0	**1,000**	100	**100**
May 7, 1987	**0**	0	100	**100**	0	0	**0**	0	**0**
Nov. 6, 1987	**0**	0	0	**0**	0	0	**500**	50	**50**
Sept. 23, 1990	**0**	0	0	**0**	0	0	**1,000**	100	**100**
Aug. 12–13, 1991	**100**	0	0	**0**	0	0	**0**	0	**0**
Sept. 7, 1991	**0**	0	0	**0**	0	1,000	**1,000**	0	**0**
Feb. 12–15, 1992	**42,300**	8,070	4,300	**12,400**	0	400	**400**	0	**0**

Table 1-3. Measured and Estimated Volumes (in Cubic Meters) of Streamflow and Infiltration Losses for the Four Reaches of Fortymile Wash (continued)

Date	Volume (m^3) [1 m^3 = 35.3 ft^3]								
	Estimated Fortymile Canyon Infiltration Loss*	Measured Narrows Gage (10251250)	Estimated Upper Jackass Flats Tributary Inflow	Estimated Upper Jackass Flats Infiltration Loss	Measured J-13 Gage (10251255)	Estimated Lower Jackass Flats Tributary Inflow	Estimated Lower Jackass Flats Infiltration Loss	Measured Amargosa Valley Gage (10251258)	Estimated Amargosa Desert Infiltration Loss
Mar. 30–31, 1992	**14,100**	0	100	**100**	0	400	**400**	0	**0**
Jan. 17–19, 1993	**51,800**	24,700	37,900	**62,600**	0	0	**0**	0	**0**
Feb. 9, 1993	**17,300**	0	0	**0**	0	0	**0**	0	**0**
Feb. 23, 1993	**10,400**	0	0	**0**	0	0	**0**	0	**0**
Jan. 25–27, 1995	**51,800**	1,500	38,000	**39,500**	0	0	**0**	0	**0**
Mar. 11–13, 1995	**51,800**	597,000	40,700	**73,700**	564,000	0	**123,000**	441,000	**440,000**
Feb. 23–24, 1998	—	—	—	—	—	—	—	—	—

Source: Savard (1998, Table 3); Tanko and Glancy (2001).

*All infiltration loss calculations (in bold) use a 7,300 m^3/km [4.2 × 105 ft^3/mi] streamflow volume loss factor (Savard, 1998) loss factor of 7,300 m^3/km [4.2 × 10^5 ft^3/mi], estimated from streamflow volume and distance traveled data (Savard, 1998). Because of the infrequent occurrence of streamflow throughout the drainage system, the hydrologic and hydraulic attributes are difficult to characterize. Even during flood events, bank-to-bank streamflow may not occur in many sections of the wide-channeled drainage system. Since recharge from streamflow was found to be relatively small, operation of the Fortymile Wash gaging stations was reduced to a low priority in the late 1990s and the stations were decommissioned (CRWMS M&O, 2000; Glancy and Beck, 1998; Tanko and Glancy, 2001).

1.4.3 Modeling Sediment Transport in Natural Streams: Applications to Fortymile Wash, Yucca Mountain, Nevada

The physics of sediment transport is complex. A thorough treatment of the hydraulics of sediment transport can be found in Graf (1971), while the mechanics of sediment-laden flows is succinctly addressed by Julien (1998). The difficulty lies in describing the mechanics of a two-phase flow of water and sediment. The interface between flowing mixtures of water and sediment particles is complicated by the unstable nature of many natural streambeds. Fine particles are brought into suspension when turbulent velocity fluctuations are large enough to maintain the particles within the mass of fluid without frequent contact with the bed. Clay and silt particles generally enter suspension. Noncohesive bed particles enter motion as soon as the shear stress applied on the bed material exceeds the critical shear stress. Therefore, when hydraulic forces exerted on sediment particles exceed the threshold condition for beginning motion, coarse sediment particles move in contact with the bed surface. Generally, sand- and gravel-sized particles roll and slide in a thin layer near the streambed. This bed load is considered a minor component of the total sediment load (usually less than 15 percent) (Knighton, 1998), but most measurements are from perennial rivers in temperate climates rather than dryland streams.

Direct methods of quantifying fluvial sediment discharge include suspended sediment sampling, bed material sampling, and bed load sampling. Concentrations of suspended load and bed load can vary significantly as flow conditions range from dilute discharge to dense concentrations almost verging on a debris flow. However, because the difficulties of bed load measurements are exacerbated by the ephemeral nature of the flow regime, our understanding of the bed load dynamics of dryland rivers lags behind that of suspended sediment (Powell, et al., 1996). Equipped with a thorough sampling strategy, the bed load database collected by Laronne and Reid (1993) and Reid, et al. (1995) in the Nahal Yatir (Negev Desert, Israel) represent some of the first measurements collected during flash floods in desert gravel-bed streams. These studies report that bed load sediment transport for this ephemeral stream is as much as 400 times more efficient at transporting coarse material than its perennial counterparts in humid climates. Estimates of bed load activity have largely been inferred from geomorphic reconstructions of recent floods using combinations of synthetic hydrographs, estimates of scour and fill, fan deposits, particle tracing studies, and predictive formulae (e.g., Knighton, 1998; Komar, 1988; Leopold, et al., 1964; Schick and Lekach, 1993).

Without direct suspended load and bed load sampling, equations based on incipient motion or energy are typically used to quantify fluvial sediment discharge. Unfortunately, these formulations require discharge measurements and knowledge of size distributions and depth-integrated sediment concentrations. No one approach is likely to describe the fundamental relationships between stream discharge, sediment transport, and particle entrainment in a dryland drainage system.

1.5 Overview of Erosion at Yucca Mountain, Nevada

Running water is still the primary agent for sediment transport in a dryland setting, but it may be limited to widely-spaced episodes. Chemical weathering and mass movements, such as creep, are dominant geomorphic processes in humid climates. These processes play a less significant role in an arid climate. Conversely, desiccation and wind action, such as deflation, are more consequential in an arid region than in a humid region.

Yucca Mountain is a faulted, east-dipping cuesta of Miocene tuffs. Overall, the erosion rate for the arid Yucca Mountain region is low compared to other environments (DOE, 1993; Whitney and Harrington, 1993; Coe, et al., 1997). Hillslopes in the area are a combination of exposed bedrock and bedrock mantled by coarse-grained, bouldery colluvium and fine-grained eolian deposits. The boulder deposits commonly are coated with a dark rock varnish, and the minimal vegetation cover provides little resistance to erosion caused by intense precipitation and the resultant runoff. Varnished colluvial surfaces are believed to represent stable surfaces. With hillslopes lacking an abundance of readily available sediment for transport, the Yucca Mountain area can be considered sediment starved. A fresh blanket of tephra could create a transport-limited condition meaning the supply of sediment exceeds the rate at which it can be transported.

1.6 Overview of Yucca Mountain Basaltic Volcanism and Analog Volcanoes

Basaltic strombolian eruptive activity, the type of activity most relevant to potentially disruptive magmatism at Yucca Mountain, is characterized by mildly explosive bursts of solidified and partly solidified ash {< 2 mm [0.08 in]}, lapilli (or cinders) {2–64 mm [0.08–2.5 in]}, and blocks and bombs {> 64 mm [2.5 in]}. When transported through the air, this volcanic ejecta is collectively termed tephra. Strombolian eruptions may range from weak to violent, depending on the magnitude of mass-flow rate and tephra dispersal. More violent explosions tend to produce smaller fragments although basaltic tephra is generally coarser grained than fine-ash-dominated silicic tephra (e.g., Walker, 1973; Cas and Wright, 1987). After an eruption, tephra could be deposited over hundreds to perhaps thousands of square kilometers [tens to perhaps thousands of square miles] around and downwind from the vent. Historically-active basaltic volcanoes with cone and tephra-fall characteristics similar to examples from the Yucca Mountain region have tephra-fall deposits roughly twice the volume of the cone (NRC, 1999). Scoria cones occur in groups or clusters in which individual cones may overlap one another. Strombolian eruptions are generally basaltic or near-basaltic in composition and may be accompanied by the ejection of relatively fluid lava spatter and the simultaneous effusion of lava. The grain-size distribution; direction, thickness, and extent of the tephra-fall deposit; and the tendency of scoria cones to occur in groups, all have important ramifications for understanding issues related to potential igneous activity at Yucca Mountain.

Few data relevant to airborne transport, dispersal, and subsequent redistribution processes are obtainable from the Yucca Mountain area. The youngest volcano in this area is 80,000-year-old Lathrop Wells (Heizler, et al., 1999), a scoria cone located in southern Yucca Mountain, less than 20 km [12.4 mi] from the potential repository footprint. The cone has a present height of about 140 m [459 ft]—there is active quarrying along the south margin—and is elongated in the north-south direction. The cone has an alkali-basalt composition, and the outer cone slopes consist mostly of loose scoria lapilli (Figure 1-2a). The physical volcanology of the Lathrop Wells volcano is summarized in Bechtel SAIC Company, LLC. (2003c,d). Noteworthy is the discovery that almost the entire tephra deposit has been eroded away, but the initial volume has been estimated to be 4×10^7 m^3 [1.4×10^9 ft^3] (NRC, 1999; Bechtel SAIC Company, LLC., 2003c,d).

Information obtained from analog volcanoes contributes to our understanding of possible future volcanism at Yucca Mountain. Observations and data obtained from the scoria cone volcanoes Parícutin (Mexico), Sunset Crater (Arizona), and Cerro Negro (Nicaragua) are utilized in this report.

1.6.1 Parícutin, Mexico

Parícutin volcano, Michoacán, Mexico, began erupting on February 20, 1943, and ceased activity on March 4, 1952. The eruption occurred on a high volcanic plateau at an elevation of approximately 2,400 m [7,874 ft]. The climate is humid subtropical with a mean annual temperature of about 15 °C and a mean annual precipitation between 1,800–2,000 mm [71–79 in], depending on elevation (Mosiño-Alemán and García, 1974; Inbar, et al., 1994). Surrounding terrain, including older volcanoes, is generally covered by a dense forest; the plains are often cultivated. The eruption of this scoria cone volcano was well documented and the case history is an acceptable analog for tephra removal processes that may occur following a possible eruption in the Yucca Mountain region.

Segerstrom (1966, 1961, 1960, 1950) made extensive observations of tephra erosion at Parícutin. He addressed the degree of compaction, redeposition, and stripping of the tephra deposit; the amount of new plant growth on lava flows and tephra falls; and the overall deceleration of erosion by 1965. Segerstrom (1961) noted that erosion and redeposition in the Parícutin area slowed for two principal reasons: (i) the most vulnerable deposits in stream channels and on the steepest slopes were largely stripped away and (ii) areas covered by tephra or new alluvial deposits were rapidly vegetated. In his final publication on the aftermath of the eruption, Segerstrom (1966) concluded that by 1965 an approach toward erosional stability was evident in the devastated area. Where the forest was not killed by the eruption, stabilization of the tephra deposit was even more rapid. The compilation by Luhr and Simkin (1993) provides a thorough overview of Parícutin, including eruption history, human response, environmental effects, and geological studies.

1.6.2 Sunset Crater, Arizona

Sunset Crater is in the San Francisco volcanic field of north-central Arizona on the southern margin of the Colorado Plateau (Figure 1-2b). The climate at Sunset Crater is semiarid (Sellers and Hill, 1974), more comparable to Yucca Mountain than the climate for Parícutin. Eruptive activity began less than 1,000 years ago in 1064 or 1065 A.D. (Smiley, 1958) and continued, probably intermittently, for about 150 years (Holm and Moore, 1987; Tanaka, et al., 1990). Proximal tephra thickness is greater than 5 m [16.4 ft], and traces of the deposit are still present 20 km [12.4 mi] from the vent (Amos, 1986), indicating that substantial tephra deposits can persist for 1,000 years even with a period of accelerated erosion immediately following the

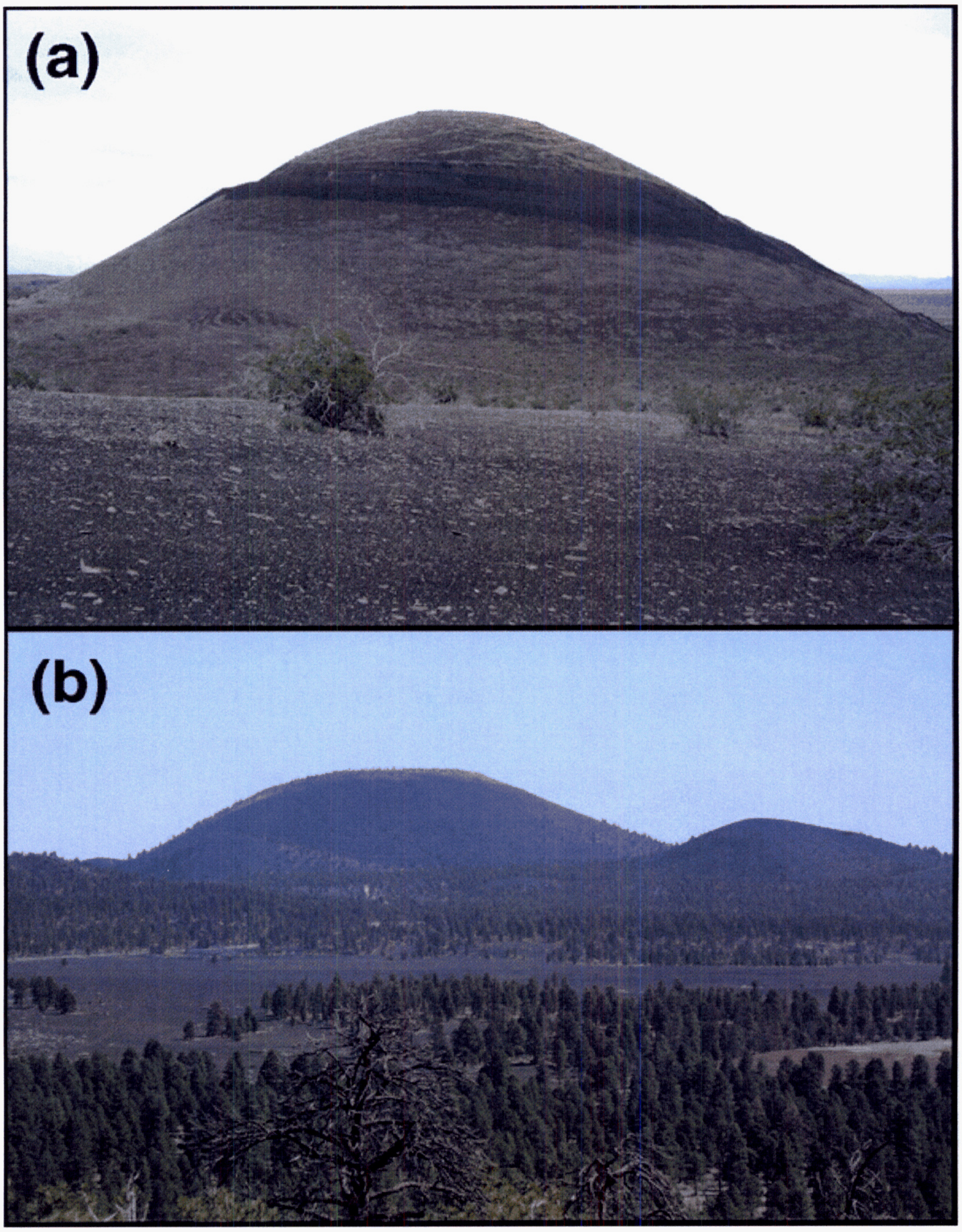

Figure 1-2. (a) Lathrop Wells Scoria Cone Viewed from the Northwest. (b) Sunset Crater Scoria Cone Viewed from the South. At Sunset Crater, the Black-Colored Tephra Deposit is Recognizable Draping the Surrounding Landscape.

eruption. There is less gullying and overland flow on Sunset Crater tephra-fall deposits than at Parícutin due to a more permeable deposit and substrate. In this case, the substrate (the material beneath the Sunset Crater tephra deposit) is also relatively permeable.

1.6.3 Cerro Negro, Nicaragua

Cerro Negro, Nicaragua, has erupted 23 times since the volcano first formed in 1850 (Simkin and Siebert, 1994). The climate at Cerro Negro is tropical with a mean annual rainfall roughly between 1,000 to 2,000 mm [39 to 79 in]. Field observations at the volcano show little evidence of overland flow or rilling on recent tephra deposits. The underlying cone and lavas, as well as the recent tephra deposit, are relatively permeable. This is in contrast to Parícutin, which experienced widespread rilling in the first 5 to 10 years after the eruption (Segerstrom, 1960). Hill, et al. (1998) used a convective-dispersive model to evaluate tephra-deposit thickness measurements recorded immediately after the 1995 scoria-cone eruption. This model was found to reasonably calculate tephra-fall thickness between 8 and 30 km [5 to 18.6 mi] from the vent and is a viable tool for tephra-fall hazard assessment. With Cerro Negro as the focus, Connor, et al. (2001) advanced a probabilistic hazard assessment for tephra fallout.

1.7 Sediment Budget Approach for Modeling the Redistribution of Tephra in Fortymile Wash, Nevada

1.7.1 Background and Definition

Emplacement of tephra-fall deposits can disrupt sediment and water routing in watersheds. The geomorphologic and hydrologic response to such a landscape disturbance may be particularly significant and prolonged, resulting in posteruption sediment yields that exceed preeruption yields (Major, et al., 2000). A large amount of easily eroded sediment derived from these deposits, coupled with the loss of protective vegetation, can trigger accelerated erosion and affect the supply of sediment to rivers (Segerstrom, 1950, 1961; Major, et al., 2000; Major, 2004). Because an understanding of the linkages between sediment sources, sediment volume, transport processes, and storage is essential to fully address the geomorphologic response, these problems are best approached through the construction of a sediment budget. The sediment budget concept and model is developed throughout this report.

In its simplest expression, the sediment budget of a drainage basin is a quantitative relationship that links sediment sources, transport processes, storage and remobilization, and discharge from the basin (Figure 1-3). This approach clarifies and quantifies the linkages between upstream erosion and downstream sediment yield, as well as integrates the temporal and spatial variations basin are defined and the sediment supplied from those sources is routed to and through the channel system, with due consideration given to the various opportunities for storage (Knighton, 1998). Sediment may be temporarily stored and remobilized several times before ultimately reaching the basin outlet. For example, a soil mantle, alluvial and colluvial deposits, channel-fill of transport and storage processes. In this approach, the various sediment sources within a deposits, and river bars may all store sediment temporarily. Each component (e.g., sediment yield, storage, discharge from basin) of a sediment budget should be quantified, mass should be balanced, and recurrence intervals for key processes should be calculated even though they may be limited by short record length or incomplete data.

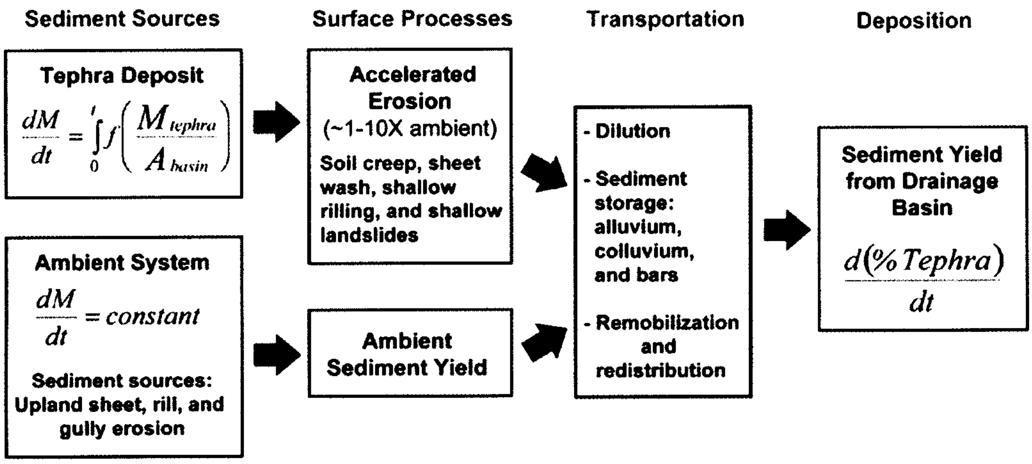

Figure 1-3. Sediment-Budget Conceptual Model Tailored for Fortymile Wash Following a Potential Tephra-Fall Deposit

Sediment yield at the basin outlet is commonly much less than the gross erosion on its upstream watershed. Temporary stores of sediment, such as colluvium, alluvium, and gravel bars, are often extensive. Therefore, sediment yield is generally measured at the mouth of the basin and is usually expressed in units of mass per unit area or volume per unit area. The difference between erosion and sediment yield is termed the sediment delivery ratio, and while such terms as denudation, sediment yield, and rate of erosion are similar, they are not necessarily synonymous. Furthermore, it is commonly observed that both sediment yield per unit area and sediment delivery ratio decrease from small to large basins (Walling and Kleo, 1979). If the sediment delivery ratio equals 1.0, the amount of material removed from hillslopes equals the amount leaving the basin as fluvial sediment yield. Because of the lack of data regarding erosion rates and fluvial sediment yield in arid or dryland basins, these sediment delivery ratios can only be estimated (Walling and Kleo, 1979).

The sediment budget approach was developed in the late 1970s. Early studies focused on the basic problem of quantifying how sediment moves through landscapes (Swanson, et al., 1982). A few examples of prominent works from this period include an early study by Leopold, et al. (1966), who measured rates of slope and channel processes in a semiarid region of New Mexico to aid analysis of arroyo filling and cutting. Dietrich and Dunne (1978) analyzed sediment transport for the deeply dissected Rock Creek basin in the Coast Range of Oregon and were particularly interested in changes in soil and sediment properties. They presented a qualitative description of sediment production and transport processes and calculated a quantitative sediment budget for this perennial system. Dietrich, et al. (1982) suggest basic rules for developing a sediment budget with examples from the forested coastal mountains of Washington and Oregon. Lehre (1982), emphasizing slope processes, made detailed measurements of erosion and sediment discharge in the small drainage basin of Lone Tree

Driftless Area of southwestern Wisconsin to compute a sediment budget based on changes in sediment storage because of the availability of abundant historical data over a period of dramatic change in sedimentation processes. These studies demonstrate that most work focuses on forested drainage basins rather than ephemeral dryland systems. Dryland systems, therefore, need more development in this report.

1.7.2 Sediment Budget Studies for Dryland Streams and Volcanic Terrains

Few sediment budget studies focus on dryland streams or volcanic deposits. Renard (1972) and Renard and Laursen (1975) propose a combined model to estimate sediment yield from small dryland drainage basins. Their model incorporates a deterministic sediment transport relationship with a stochastically defined runoff component, but does not produce a true sediment budget that accounts for mass balance within the drainage system. The installation of fully automated sediment monitoring stations on Nahal Eshtemoa and Nahal Yatir, two ephemeral channels in the Negev Desert, Israel, provides detailed insights into the sediment transport dynamics of dryland streams (Powell, et al., 1996; Reid, et al., 1998; Reid, et al., 1995). These stations allow total sediment load to be calculated to a high degree of certainty by independently measuring suspended sediment concentration and bed load during flash floods. Powell, et al. (1996) stress hydrological response and sediment transport in this system rather than surface processes and erosion, but all necessary components are present in their work to produce a sediment budget. They also note the extreme inter- and intra-annual variability of sediment transport in ephemeral streams that make the evaluation of sediment yield for drylands especially problematic, particularly for predicting long-term patterns.

Parícutin (1943–1952) is a historic scoria cone produced by a violent strombolian eruption. Although this volcano receives approximately 12 times the annual precipitation of Yucca Mountain, it is a reasonable analog because of the eruption type, nature of the deposit, and thorough documentation of subsequent erosion. Unlike either Sunset Crater (Arizona) or Cerro Negro (Nicaragua), the Parícutin tephra deposit has extensive rilling, and the underlying older cones and lavas are relatively impermeable. The rates and processes observed and measured at Parícutin, therefore, are not directly transferable to the Yucca Mountain region. Regarding specific studies, Segerstrom (1961) and Inbar, et al. (1994) diagrammatically represented erosion rates, expressed as a relative sediment yield (or relative volume of material eroded), for the tephra-covered region at Parícutin. (Posteruption sediment yield is discussed in Chapter 4.) However, neither study produced a sediment budget or similar quantitative expression of erosion and redistribution of tephra.

A widespread landscape disturbance by the catastrophic 1980 eruption of Mount St. Helens, Washington, abruptly increased sediment supply in surrounding watersheds. Continuous monitoring of streamflow and suspended-sediment discharges from disturbed basins following this eruption reveals when, and under what conditions, sediment redistribution occurs following a major landscape disturbance. Lehre, et al. (1983) calculated the posteruption sediment budget for the North Fork Toutle River drainage, June 1980–June 1981, at Mount St. Helens. Simple field and air-photo measurements were used to assess the quantity and distribution of sediment. Major (2004) and Major, et al. (2000) composed a two-decade perspective of annual sediment yield from gaged drainage around Mount St. Helens. These studies did not attempt to achieve mass balance for the Toutle River drainage system, but documented an initial post-eruption sediment yield exceeding the preeruption yield by several orders of magnitude because of erosion of the voluminous debris-avalanche deposit. Watersheds proximally north of the volcano, which were most affected by the directed blast, underwent the most severe disturbance because of the large debris avalanche. This primarily comprises the upper North Fork Toutle River valley. Suspended-sediment yields from two lahar-affected basins (South Fork Toutle River and Muddy River) are substantially less than from the avalanche deposit. The Green River, affected solely by the lateral blast and thin tephra deposits, transported the least suspended sediment. Major (2004) and Major, et al. (2000) conclude that twenty years after the catastrophic eruption at Mount St. Helens, suspended-sediment yields remain 1 to 2 orders-of-magnitude above background levels in basins where mass-flow sediments were deposited in channels. In basins where the geomorphic impact was dominantly hillslope disturbance (e.g., Green River basin), suspended-sediment yields returned to background levels within five years. As these studies attest, Mount St. Helens produced tephra-fall, debris avalanche, and lahar deposits. The grain-size characteristics are different for each of these and likely erode by processes other than a basaltic tephra-fall deposit. Therefore, most of Mount St. Helens has little analogy to Yucca Mountain processes.

Chinen and Kadomura (1986) produced a posteruption sediment budget for a small catchment on Usu volcano in Hokkaido, Japan. The 1977–1982 eruption of this stratovolcano deposited tephra in the summit region, which was promptly eroded by sheet wash, rill, and gully processes, as well as minor periglacial activity. Channel-fill and colluvial deposits accounted for the majority of sediment storage. They note a 1- to 2-year time lag between sediment production and yield, but tilting, faulting, and dome-growth activity was affecting the small study catchment basin. Sediment yield declined rapidly three years after the latest tephra-producing eruption, but construction of erosion-control works terminated the study.

Following an eruption, easily erodible sediment and the destruction of protective vegetation create extremely high sediment yields in rivers draining volcanic terrains. Nevertheless, studies of Cascade volcanoes or the Negev Desert are poor analogs for a potential tephra deposit in the Yucca Mountain region following renewed volcanic activity. The extent and character of erosion at each location is a complex function of site-specific processes and characteristics.

2 FLOOD FREQUENCY IN FORTYMILE WASH

2.1 Technical Basis

The objective of this flood-frequency analysis is to support the calculation of sediment yield in Fortymile Wash. The frequency and magnitude of flood and streamflow events controls how sediment is routed through dryland river systems. By analyzing the frequency of floods of various sizes, a recurrence interval can be developed for a river or stream at a specific locality. The recurrence interval is the average time interval between floods of a particular size and is the reciprocal of flood probability:

$$R.I. = \frac{1}{P} \quad (2\text{-}1)$$

where *R.I.* is the recurrence (or return) interval of the flood of the same magnitude, and *P* is the probability of a given flow magnitude being equaled or exceeded in a single year.

A graph presenting annual flood magnitudes plotted against recurrence interval is a flood-frequency curve. The simplest plotting formula, the Weibull equation (e.g., Costa and Baker, 1981; Graf, 1988; Ritter, et al., 2002), calculates the recurrence interval by taking the average time between two floods of equal or greater magnitude:

$$R.I. = \frac{n+1}{M} \quad (2\text{-}2)$$

where *n* is the number of discharge values, usually the number of years in an annual series, and *M* is the magnitude order number of the sample (the largest flood in *n* years is assigned *M* equals 1, the second largest flood *M* equals 2, and so forth). Large, catastrophic floods generally have a low frequency of occurrence, and by this formula a flood with a 0.01 or 1 percent probability of occurring in a year has a recurrence interval of 100 years. Similarly, the probability of a 50-year flood (or *R.I.* equals 50 years) occurring in any given year is 0.02 or 2 percent.

A flood-frequency relationship for both gaged and ungaged streams that drain dryland basins is complex because rainfall is variable in time and space and the physiography of each drainage basin is extremely variable. The mean annual flood has almost no practical or theoretical significance in dryland rivers because of the extreme variability of flow in such streams (Graf, 1988). The development of accurate flood-frequency plots is unlikely in many arid basins because of short record length and the variability of annual peak discharges. At some sites (including Fortymile Wash), most years have no flow. At other sites, commonly used probability distributions do not appear to fit the plot of annual peak discharges (Thomas, et al., 1997). Although these limitations cannot be completely resolved, an alternative plotting formula by Gringorten (1963) is designed for short record lengths:

$$R.I. = \frac{n+0.12}{M-0.44} \quad (2\text{-}3)$$

where all terms have previously been defined. This equation will be used to construct the flood-frequency curve for Fortymile Wash.

2.2 Flood-Frequency Curve

Peak discharge data measured at the Amargosa Valley gage (Station Number 10251258), Fortymile Wash, are listed in Table 1-2. Of the three gaging stations along the main channel of Fortymile Wash, this site is located the farthest south at the intersection of the southern boundary of the Nevada test site and the wash (Figure 1-1). This is also the most important gaging station for recording the movement of sediment down the wash and towards the reasonably maximally exposed individual location (Bechtel SAIC Company, LLC., 2003a). Streamflow data for Fortymile Wash span 30 years, 1969 to 1998. Most years have no recorded streamflow, but three years (1969, 1984, and 1987) have multiple floods. The August 14–16, 1984, flood is not used because no peak discharge measurement was recorded and it occurred the same week as another larger flood. If a strict annual series of measurements is maintained (i.e., $n = 30$), these three critical data points would be lost. Therefore, for this special case of an ephemeral stream in a dryland basin, the time period will be 30 years, and all 11 measured flood events will be used in the analysis. It is assumed these are the largest floods over this 30-year period. After rainfall or snowmelt, streamflow may be recorded locally at one or more of the three Fortymile Wash gages, but usually not continuous from gage to gage. This local or tributary flow, most often noted in the upper Fortymile Wash drainage basin, may be small in volume and infiltrate before reaching the final, southernmost gage near U.S. Highway 95 (Station Number 10251258). There are several examples of such small-volume, localized streamflow within sub-basins of Fortymile Wash (e.g., Savard, 1998, 1996, 1995; Waddell, et al., 1984), indicating episodes of sediment transport and storage, but not discharge from the Fortymile Wash drainage system. Furthermore, the upstream reaches and tributaries of Fortymile Wash were not gaged until 1983 (Glancy and Beck, 1998; Waddell, et al., 1984) (Table 1-1). Many of these same streamflow gages, installed by the U.S. Geological Survey in cooperation with DOE, were deactivated by the late 1990s because of funding cuts (Glancy and Beck, 1998).

Estimates for 100-year and 500-year floods in the Fortymile Wash drainage system are from Squires and Young (1984). They used the records of 12 gaging stations adjacent to the Nevada Test Site to estimate 100-year and 500-year flood magnitudes for Fortymile Wash, as well as its principal southwestern tributaries, Busted Butte (now Dune), Drill Hole, and Yucca Washes. Their estimate of the peak discharge for a 100-year flood in Fortymile Wash is 340 m^3/s [12,000 ft^3/s] and for a 500-year flood is 1,642 m^3/s [58,000 ft^3/s]. With such a short record length, the plotting formula by Gringorten (1963) [Eq. (2-3)] is used to calculate the recurrence interval. The estimated 100-year and 500-year floods are neither plotted nor ranked, but are valuable for comparison. Flood dates, peak discharge, rankings, recurrence interval, and a comparison to the standard Weibull method are cataloged in Table 2-1. The flood-frequency curve is shown in Figure 2-1. The limitation to this curve is that the flood-frequency analysis is based on a very short period of record with only 11 measured data points. The estimated 100-year and 500-year floods could be included in this calculation, but it would be extending these data beyond the period of record. These limitations are common for dryland streams, where peak discharge events often have not been recorded. Thus, the flood-frequency curve reflects a large uncertainty in recurrence rate.

Table 2-1. Peak Discharge, Rankings, and Recurrence Intervals for the Amargosa Valley Gage (Station Number 10251258), Fortymile Wash, Yucca Mountain, Nevada				
Date	**Peak Discharge (m^3/s)***	**M (Rank)**	**Recurrence Interval (yr) [Weibull]**	**Recurrence Interval (yr) [Gringorten]**
January 25, 1969	42.5	2	15.5	19.2
February 24–26, 1969	93.5	1	31	53.6
March 3, 1983	11.3	5	6.2	6.6
July 21–23, 1984	40.5	3	10.3	11.7
August 18–20, 1984	10.5	6	5.2	5.4
July 19–20, 1985	0.09	8	3.9	4.0
February 23, 1987	0.02	9	3.4	3.5
November 6, 1987	0.02	11	2.8	2.8
September 23, 1990	0.02	10	3.1	3.1
March 11–13, 1995	34.0	4	7.8	8.4
February 23–24, 1998	9.6	7	4.4	4.6
Estimated 100-yr flood†	340	N/A	N/A	N/A
Estimated 500-yr flood†	1,642	N/A	N/A	N/A

*1 m^3/s = 35.3 ft^3/s
†Source: Squires, R.R. and R.L. Young. "Flood Potential of Fortymile Wash and its Principal Southwestern Tributaries, Nevada Test Site, Southern Nevada." U.S. Geological Survey Water-Resources Investigations Report 83–4001. p. 33. 1984.

Eleven flood events have been recorded at the Amargosa Valley gage over a 30-year period from 1969 to 1998. On average, this is a flood every 2.7 years. However, several of these floods have a peak discharge of less than 1 m^3/s. When using the seven largest floods, this average increases to 4.3 years between floods. Therefore, the time between flow events is about 4 years. This simple reasoning defines the TPA code parameter TimeBetweenFlowEvents[yr] (Benke, et al., 2005), which is assigned a value of 4 years. Furthermore, by applying a linear curve fit to the flood data and assigning $x = 4$ for a recurrence interval of 4 years, the following equation from Figure 2-1 is another method to examine flood frequency:

$$y = 1.54 + 1.83 \text{ x } 4 = 8.86 \qquad (2\text{-}4)$$

where every four years a flood of 8.86 m^3/s [313 ft^3/s], roughly equal to the February 1998 flood, could be expected.

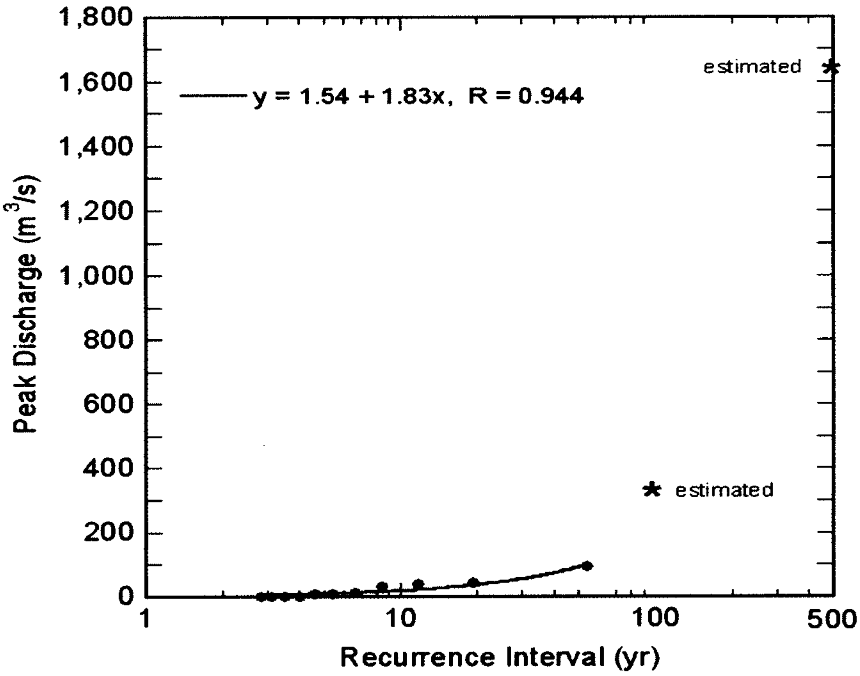

Figure 2-1. Flood-Frequency Curve for Fortymile Wash at the Amargosa Valley Gage (Station Number 10251258)

The recurrence intervals listed in Table 2-1 provide one final insight regarding flood periodicity and risk, whereby the February 1969 flood has been the largest one measured thus far in Fortymile Wash—it is only a 30-year or 50-year flood. A larger flood, which may affect settlements, roads and highways, evacuation plans, and agriculture (Amargosa Farms), is expected in the future . The potential impact to facilities and construction related to potential high-level waste storage at Yucca Mountain previously has been addressed (e.g., Bullard, 1992; Glancy, 1994; Glancy and Beck, 1998; Squires and Young, 1984).

3 SEDIMENT YIELD AND MASS OF ERUPTED TEPHRA

3.1 Tephra Dispersal Parameters for Redistribution

The simulation of aerial transport of material from an erupting volcano is used to calculate the initial deposition of tephra in the Fortymile Wash catchment basin and the initial deposition of tephra at the reasonably maximally exposed individual. The ASHPLUME computer code was developed for atmospheric dispersion and subsequent deposition of tephra from a potential eruption at Yucca Mountain, Nevada (Jarzemba, et al., 1997). The ASHPLUME conceptual model subsequently was modified into the code TEPHRA,[1] which calculates potential tephra deposit distributions using realistic, stratified wind fields based on actual upper atmosphere data from Desert Rock, Nevada (National Oceanic and Atmospheric Administration, N.D.). For example, ten 1-km [0.62-mi] height bins are used to simulate a stratified wind field in the Yucca Mountain area. With the current, validated version of TEPHRA, deposits for the 1995 Cerro Negro eruption in Nicaragua can be calculated using model parameters collected during that eruption (Hill, et al., 1998). By employing parallel computer processing, TEPHRA allows the user to calculate expected tephra and spent nuclear fuel accumulation as a conditional probability at x, y points on a spatial grid.

ASHPLUME is a module in the TPA code. TEPHRA, however, runs as a stand-alone code outside of the TPA code. TEPHRA is used to create a data or lookup table, which can be sampled during total system performance assessment realizations. The primary benefit of a lookup table is that this approach allows the evaluation of tephra deposits and high-level waste from three sources: (i) initial deposition at the reasonably maximally exposed individual (or receptor location), (ii) fluvial redistribution, and (iii) eolian remobilization. The TPA code also was modified to include a new module for tephra remobilization and resuspension.

The TEPHRA lookup table provides values for several TPA code parameters (Benke, et al., 2005). The most important parameters for this report are the mass of tephra deposited in the Fortymile Wash catchment basin from the eruption ($M_{teph,erup}$) and the area of the Fortymile Wash catchment basin containing a tephra deposit from the eruption (A_{teph}). Statistics were generated from 1,024 realizations of the code TEPHRA using Yucca Mountain conditions for basaltic volcanic eruptions and the wind field for Desert Rock. The statistics for these parameters are recorded in Table 3-1 with the area term, A_{teph}, listed with the mean ±1σ (standard deviation) and the mass term, $M_{teph,erup}$, listed with the mean and ±2 standard deviations to encompass 95 percent of all observations. Figure 3-1 illustrates the area of the Fortymile Wash catchment basin, which is 815 km^2 [315 mi^2]. From TEPHRA, the mean value for the area of the Fortymile Wash catchment basin containing a tephra deposit from the eruption (A_{teph}) is 149 km^2 [57.5 mi^2] or 18.3 percent of the catchment basin. For comparative purposes, this is an area approximately equal to the Fortymile Wash depositional basin {136 km^2 [52.5 mi^2]}.

[1]Winfrey, B. "Software Validation Test Plan and Report, TEPHRA, Version 1.0." San Antonio, Texas: CNWRA. 2005.

Table 3-1. Tephra Redistribution Parameters for Sediment Yield and Mass of Erupted Tephra			
Parameter Name	**Description**	**Value**	**Comments**
A_{teph}	Area of Fortymile Wash catchment basin covered by tephra	149 ± 78 km^2 (mean ± 1σ)	Parameter area_f (m^2) in TEPHRA lookup table
$M_{teph,erup}$	Mass of erupted tephra in the Fortymile Wash catchment basin	2.5×10^{10} kg (mean) 8.1×10^{10} kg (+2σ) 6.9×10^{9} kg (−2σ)	Parameter m_ash_f(g) in TEPHRA lookup table
Y_{sed}	Sediment yield: a measure of sediment transport to the Fortymile Wash depositional fan	8.9×10^{6} kg/yr (mean) 1.5×10^{7} kg/yr (+2σ) 2.9×10^{6} kg/yr (−2σ)	

3.2 Sediment Accumulation Rates in the Fortymile Wash Depositional Fan

The volume of sediment deposited in the Fortymile Wash alluvial (or depositional) fan was estimated by Hill[2]. This approach begins with the observation that most of the active depositional fan consists of non-varnished to lightly varnished desert pavement. These high albedo surfaces are easily distinguished in Landsat Thematic Mapper imagery (Figure 3-2). Using this criterion, the area of the active depositional fan is 24 ± 2 km^2 [9.3 ± 0.8 mi^2]. The thickness of the recently active deposit is assumed to be 1 to 2 m [3.3 to 6.6 ft], as supported by the pattern of channel migration, bars, levees, abandoned lobes, and overall low topographic relief. Based on the satellite image data and surficial deposits described by Peterson, et al. (1995), the age of sediment accumulation in the alluvial fan is estimated between 4,000 to 10,000 years. Therefore, the depositional area, sediment thickness, and sediment age have been defined. By using a bulk density of 1,600 kg/m^3 [100 lb/ft^3] (Leopold, et al., 1966; Selby, 1993) for alluvial channel sediment, the amount of sediment transported to the Fortymile Wash depositional basin (i.e., sediment yield) is calculated. Fortymile Wash sediment yield, Y_{sed}, has a mean value of 8.9×10^{6} kg/yr [2×10^{7} lb/yr] or 7 $m^3\ km^{-2}\ yr^{-1}$ [640 $ft^3\ mi^{-2}\ yr^{-1}$]. Table 3-1 lists Y_{sed} with mean and ±2 standard deviations.

[2]Hill, B.E.. "Field Volcanism." CNWRA Scientific Notebook 088. San Antonio, Texas: CNWRA.

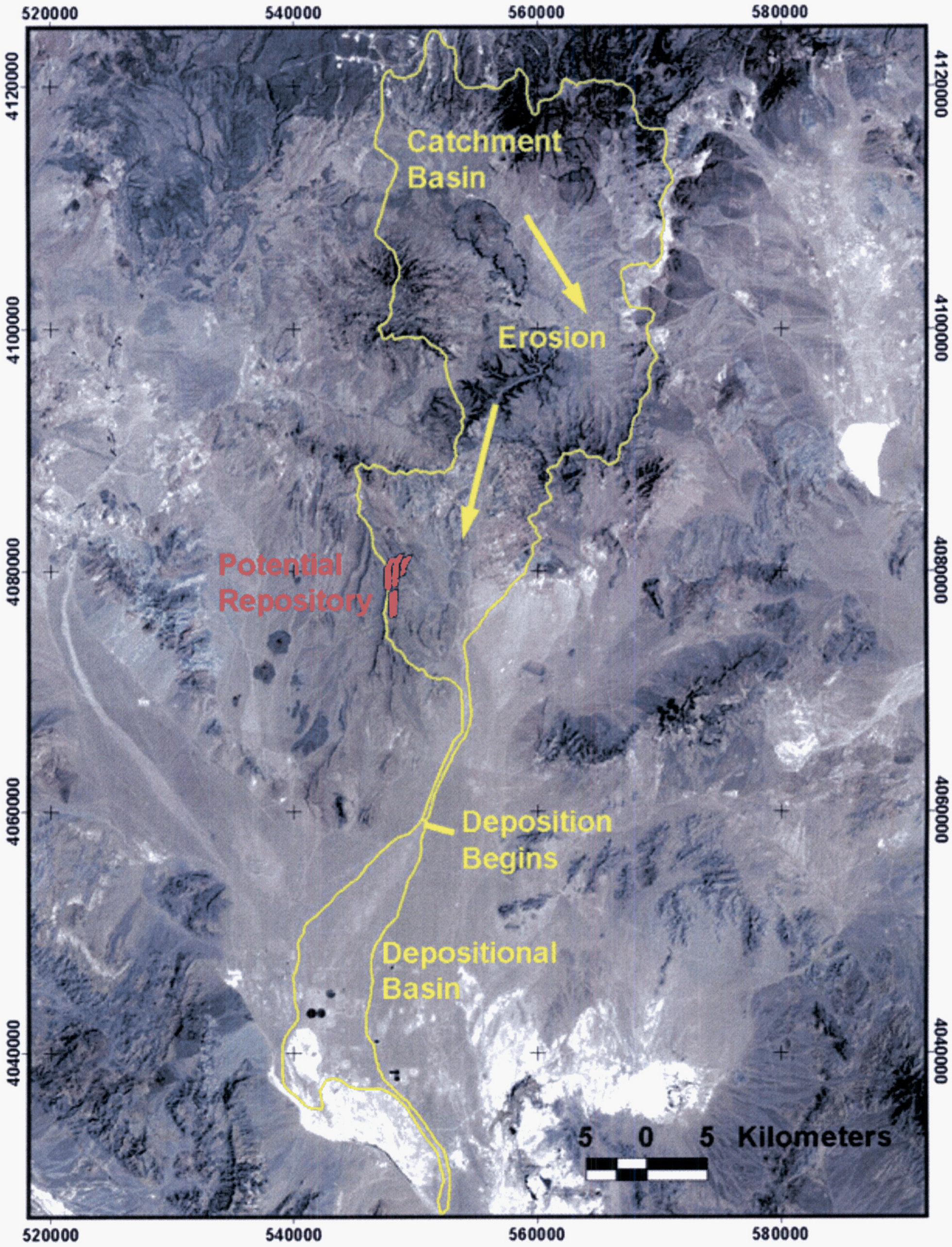

Figure 3-1. Landsat Thematic Mapper Image Showing the Fortymile Wash Drainage System. The Fortymile Wash Catchment Basin has an Area of 815 km^2 [315 mi^2] while the Pleistocene Depositional Basin has an Area of 136 km^2 [52.5 mi^2]. Erosional and Depositional Outlines Determined from the U.S. Geological Survey 7.5 Minute Topographic Maps. Map Projection: Universal Transverse Mercator, Zone 11 North, in Meters [1 m = 3.3 ft].

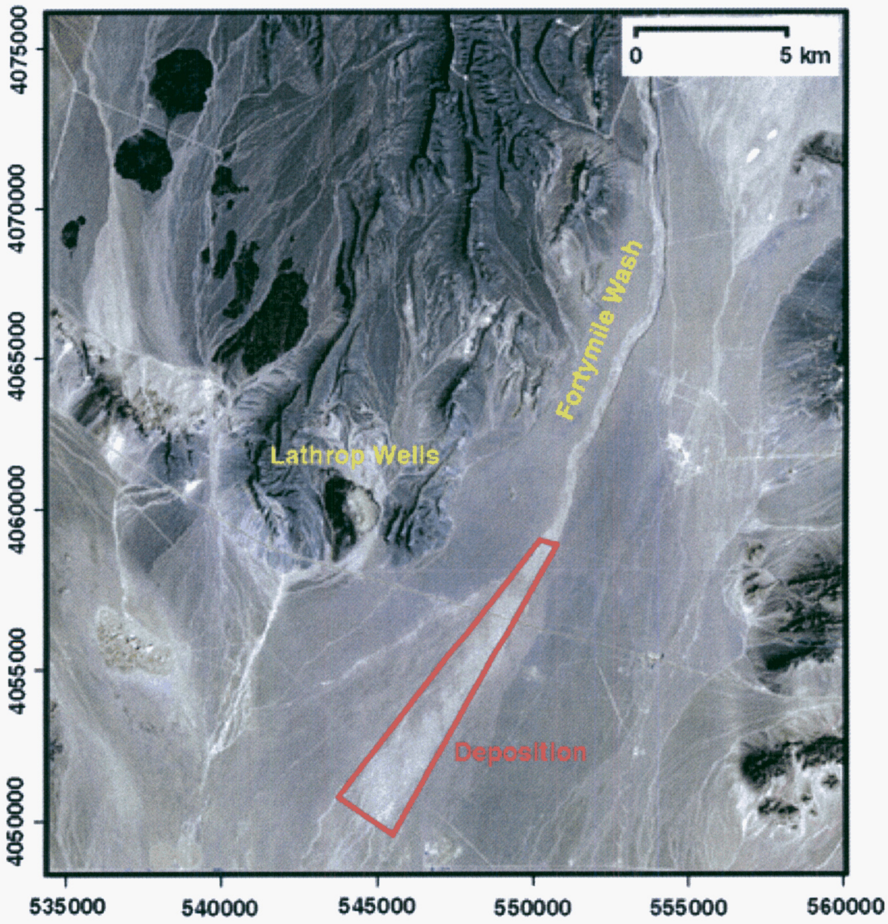

Figure 3-2. Landsat Thematic Mapper Image Showing the Active Part of the Fortymile Wash Depositional (or Alluvial) Basin in Red. Area of the Active Fan is 24 ± 2 km^2 [9.3 ± 0.8 mi^2]. Map Projection: Universal Transverse Mercator, Zone 11 North, in Meters [1 m = 3.3 ft].

4 CALCULATING POSTERUPTION SEDIMENT YIELD

4.1 Background

Explosive volcanic eruptions can disrupt the supply of sediment to rivers and perturb runoff hydrology. A large amount of easily eroded sediment derived from these deposits, coupled with the loss of protective vegetation, can trigger accelerated erosion and dramatically increase sediment yield in the aftermath of a volcanic eruption. In many ways, the effects of tephra fall are similar to the effects of erosion that result from the destruction of vegetation by fire. Several examples exist with a documented increase in sediment yield following a tephra-producing eruption, including Parícutin, Mexico (Segerstrom, 1961, 1950); Irazú, Costa Rica (Waldron, 1967); Usu, Japan (Chinen and Kadomura, 1986; Kadomura, et al., 1983); and Mount St. Helens, Washington (Collins and Dunne, 1986; Collins, et al., 1983; Major, 2004; Major, et al., 2000).

The rate at which these sediment yields rapidly increase and then decrease to preeruption levels depends upon climatic setting, terrain, and the nature of erupted material. Although they are poor analogs for a violent strombolian eruption in the Yucca Mountain region, Parícutin and Mount St. Helens are perhaps the most thoroughly documented examples. The study in which Segerstrom (1961) estimated the deceleration of erosion at Parícutin volcano ended with the year 1960 (Figure 4-1). Segerstrom, however, does not go into detail as to how he calculated or measured the data in his plot. The erosion rate peaked in 1944, the second year of the eruption, with a relative sediment yield seven times greater than the pre-eruption rate. Inbar, et al. (1994) attempted to extrapolate the Segerstrom plot, but they used manual curve-fitting. Hence, the Segerstrom (1961) data are extrapolated using a logarithmic curve fit (Figure 4-1). Based upon this extrapolation, the Parícutin area should return to a normal, preeruption sediment yield in 1972, 30 years after the start of the eruption. This is a fairly rapid return to preeruption conditions, but this area of the high, humid plateau of central Mexico receives a mean annual precipitation between 1,800 and 2,000 mm [71 and 79 in] (Inbar, et al., 1994; Mosiño-Alemán and García, 1974).

Twenty years after the catastrophic eruption at Mount St. Helens, suspended-sediment yields remain high. Major (2004) and Major, et al. (2000) concluded that sediment yields in the aftermath of explosive volcanic eruptions typically decline nonlinearly as physical and vegetative processes reduce sediment yield. In basins where the geomorphic impact was dominantly hillslope disturbance (e.g., Green River basin), suspended-sediment yields returned to background levels within five years. Therefore, Major (2004) and Major, et al. (2000) conclude that the persistence of extraordinary suspended-sediment yields from severely disturbed channels indicate that mobile supplies of sediment remain accessible, and those supplies likely will not be exhausted for many more years or possibly decades.

The rate and magnitude of accelerated erosion at Mount St. Helens, a subduction zone stratovolcano, is informative, but is not analogous to a potential scoria-cone volcano at Yucca Mountain. A plinian pyroclastic-fall deposit is from a highly explosive eruption of high-viscosity magma, generally andesitic to rhyolitic in composition. Basaltic tephra is generally coarser grained than fine-ash-dominated silicic tephra (e.g., Cas and Wright, 1987; Walker, 1973). The tephra from Mount St. Helens is not homogeneous, but is part of a complex stratigraphy with widespread ash fall, blocky debris-avalanche deposits, and pumiceous pyroclastic-flow deposits. This complex deposit has limited analogy to a potential tephra deposit at Yucca Mountain.

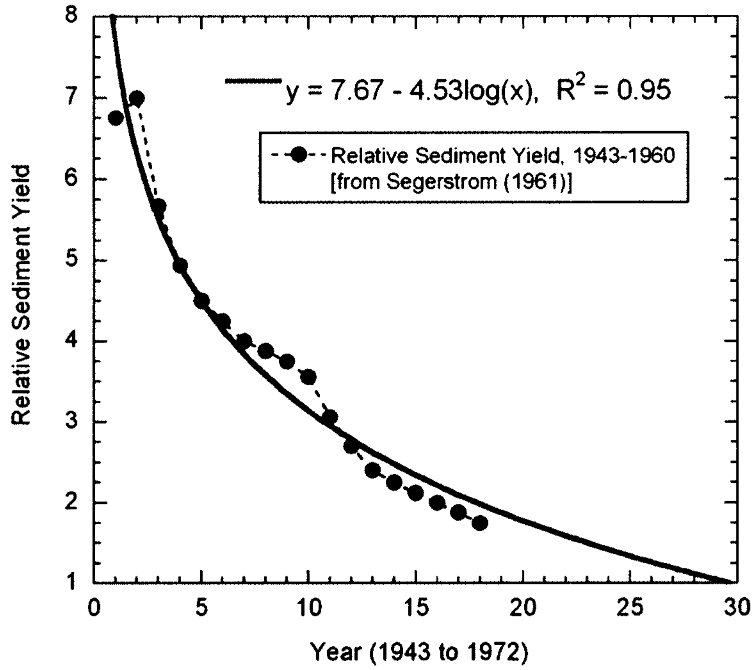

Figure 4-1. Measured Decline in Erosion Rate at Parícutin Volcano, Mexico

Therefore, an abstracted model has been developed that combines empiricism and numerical modeling in order to quantify accelerated erosion and its impact on sediment yield in Fortymile Wash following a potential tephra-fall eruption. Sediment yield is a fundamental element in the Fortymile Wash sediment budget.

4.2 Technical Basis

There are large uncertainties in quantifying the erosional history of a basaltic tephra deposit in a dryland environment because there is a lack of pertinent data. Few data relevant to tephra dispersal and redistribution processes are obtainable from the Yucca Mountain area, and data derived from analog areas with tephra deposition lack a comparable climate and volcanological character. Because of these uncertainties, a simplified approach is described to model accelerated erosion of a potential tephra deposit in the Yucca Mountain region. This approach assumes that a fresh tephra deposit drapes the landscape, maintaining the mean slope angle for the Fortymile Wash catchment basin. This condition is transport-limited, meaning the supply of sediment exceeds the rate at which it can be transported. Cumulative effects of hillslope processes that act upon this deposit of loose, unconsolidated material may be considered diffusive in that the short-range transport rate is dependent linearly on local slope (e.g., Anderson, 1994; Kooi and Beaumont, 1994). In such cases, transport can be represented appropriately by a diffusion equation. A fully-integrated, landscape-evolution model with long-term fluvial transport is beyond the objective of addressing accelerated erosion. For this model abstraction, the rate of sediment transport measured across a representative hillslope profile serves as a proxy for the erosion of the entire tephra deposit.

The procedure to compute accelerated erosion includes the following steps:

(1) Select a first-order hillslope model rule

(2) Produce a slope map and calculate the mean slope for the Fortymile Wash catchment basin

(3) Define tephra deposit characteristics using Lathrop Wells as a model for Yucca Mountain area volcanism

(4) Use a gridded profile of representative Fortymile Wash terrain to determine sediment transport and erosion

(5) Use calculated sediment transport rates to compute the relative sediment yield

The analytical models of Culling (1965, 1963, 1960) represented the first attempt to develop a mathematical theory of slope erosion with a general diffusion-like equation similar to that derived for conductive heat transfer in solids or for chemical dispersion. During the succeeding 25 years, numerous workers applied and refined these hillslope models to estimate the age of fault scarps and marine, lacustrine, or fluvial terrace scarps (Andrews and Bucknam, 1987; Andrews and Hanks, 1985; Colman and Watson, 1983; Hanks and Wallace, 1985; Hanks, et al., 1984; Mayer, 1984; Nash, 1984, 1980a,b; Pierce and Colman, 1986).

The fundamental assumption of these hillslope models is the local conservation of mass. Such continuity relations have been applied to hillslopes, notably Kirkby (1971) and Carson and Kirkby (1972), and require that an increase or decrease in the downslope flow rate of material over a straight line segment of the hillslope will cause the elevation of the segment to decrease or increase with time. Using the simpler form for one spatial dimension, this relationship can be expressed as

$$\frac{\partial z}{\partial t} = -\frac{\partial Q_x}{\partial x} \qquad \text{(4-1)}$$

where z is the vertical coordinate direction or elevation, Q_x is the material flux in the x direction, x is the horizontal coordinate direction, and t is time. The minus sign represents the transportation of mass in the downslope direction.

In the simplest case, material is moved downslope by the cumulative effects of soil creep, rain splash, freeze-thaw movements, bioturbation, shallow landslides, and shallow rilling. All hillslope processes are dictated to some degree by the local slope angle. If the downslope transport rate is assumed to be linearly proportional to the local slope, the simplest modeling rule becomes

$$Q_x = -k\frac{\partial z}{\partial x} \qquad \text{(4-2)}$$

where $\partial z/\partial x$ is the topographic gradient for a profile orthogonal to the hillslope, and k is a transport coefficient encompassing all geomorphologic processes acting on the slope.

If it is assumed that volume is conserved (porosity changes are ignored), solution is negligible, and local tectonic or isostatic readjustment is absent, then the combination of the mass flux and mass conservation equations gives the linear diffusion equation,

$$\frac{\partial z}{\partial t} = D \frac{\partial^2 z}{\partial x^2} \tag{4-3}$$

where *D*, the diffusion coefficient or mass diffusivity, reflects the long-term efficiency of sediment transport and is expected to be a function of climate and lithology. Diffusivity always has units of L^2/T. If desired, this equation can be extended to both *x* and *y* coordinate directions for the two-dimensional case, although in this work the focus will be on landforms described by a single profile, *z*(*x*). Rigorous mathematical methods of solution and a discussion of initial and boundary conditions can be found in Carslaw and Jaeger (1959) and Crank (1975).

First, the mean slope angle for the Fortymile Wash catchment basin was calculated because all hillslope processes are dictated to some degree by the slope angle. Slope is a measure of the rate of change of elevation in the direction of steepest descent. A gridded surface or digital elevation model of the drainage system was constructed from standard U.S. Geological Survey digital map products. Next, these raster data were resampled to a 30-m [98.4-ft] grid spacing or cell size using standard geographic and spatial applications. Focusing only on the Fortymile Wash catchment basin (area of 815 km^2 [315 mi^2]), the remainder of the map area was masked out, and a slope-angle map was generated (Figure 4-2). From this procedure, the mean slope angle for the catchment basin is 10.7 degrees (Table 4-1).

This information was then employed to construct a topographic grid or profile for modeling purposes. The preferred grid length is 750 m [2461 ft] comprising 25 cells with a unit cell size of 30 m [98.4 ft] to remain consistent with standard U.S. Geological Survey map products. Slope angles range from 1 degree to a maximum of 26 degrees, but the grid maintains a mean slope angle of 10.7 degrees to be consistent with the mean slope characteristics of the entire catchment basin. An additional 10 grid cells of zero slope are added to serve as the depositional basin, bringing the entire length of the topographic grid to 35 cells and 1,050 m [3,445 ft]. The profile is illustrated in Figure 4-3. This modeling grid was deliberately kept small so that it could run in a spreadsheet environment, even though this is labor intensive.

Taylor series expansion can be used to convert the diffusion equation to a finite-difference form (e.g., Crank, 1975; Harbaugh and Bonham-Carter, 1970; Richtmyer and Morton, 1967). Finite-difference models operate on a discretized space and solve for the change in some property of each cell (e.g., topographic elevation) by approximating the differential equation in a finite number of temporal steps or time increments. Finite-difference analysis simulates the movement of material into (aggradation) or out of (erosion) the cell being evaluated in a manner proportional to the elevation difference and erodibility between neighboring cells:

$$z_{t+1,i} = z_{t,i} + D \frac{\Delta t}{(\Delta x)^2} \left(z_{t,i+1} + z_{t,i-1} - 2 z_{t,i} \right) \tag{4-4}$$

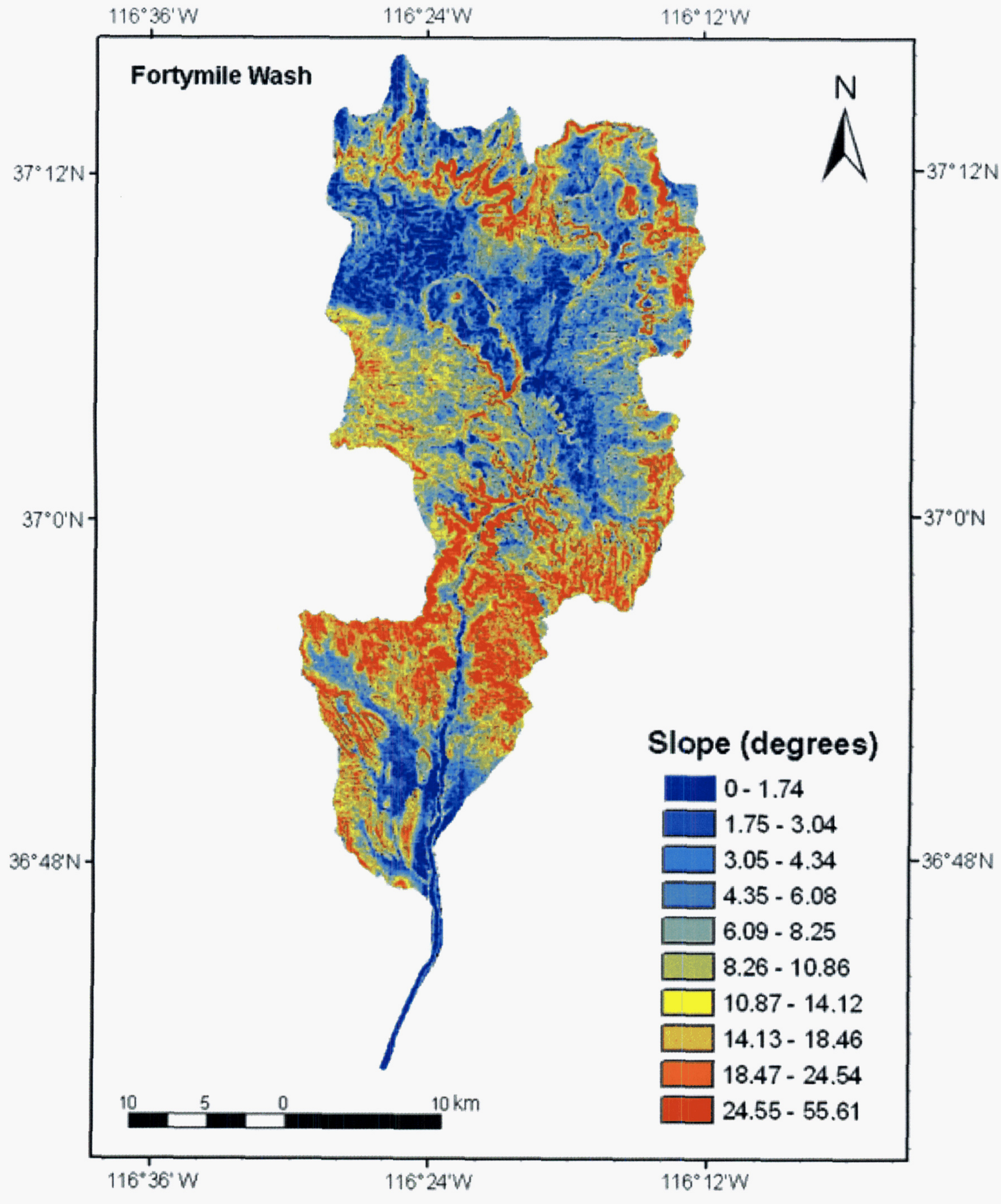

Figure 4-2. Slope-Angle Map for the Fortymile Wash Catchment Basin. Slope Angle Bins are Based on an Equal Number of Samples Rather Than Equal Bin Intervals. [1 km = 0.62 mi].

Table 4-1. Classification Statistics for the Fortymile Wash Slope Map	
Statistic/Parameter	**Value**
A_{fmw} (Area of Fortymile Wash Catchment Basin)	8.15×10^8 m^2
Grid Cell Size	30 m × 30 m
Number of Cells (Count)	905,909
Minimum Slope	0 Degrees
Maximum Slope	55.6 Degrees
Mean Slope	10.7 Degrees
Standard Deviation	8.9 Degrees

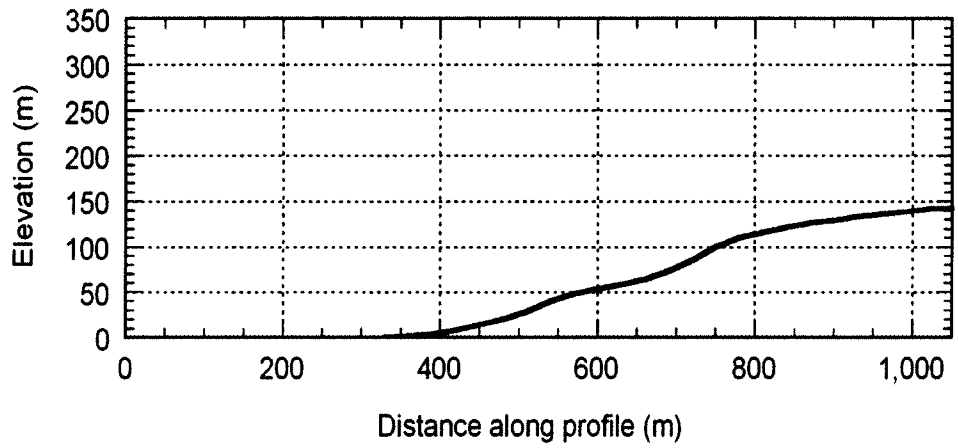

Figure 4-3. Profile of the Topographic Grid Used for Calculating Accelerated Erosion. The Grid Depicts Mean Topography (Slope Angle) Across the Entire Fortymile Wash Catchment Basin. The Profile is 1,050 m [3,445 ft] in Length and Includes 300 m [984 ft] (or 10 Grid Cells) of Zero Slope Angle for Deposition (on Left of Grid).

where $z_{t,i}$ is the topographic elevation at grid cell i at time t, $z_{t+1,i}$ is the topographic elevation at cell i at time (t + 1) (and so forth for other combinations of subscripts), D is the diffusion coefficient or mass diffusivity, Δt is the time increment, and Δx is the distance increment in the horizontal coordinate direction. This method produces an unstable solution, but the time increment can be kept sufficiently small to prevent the amplification of errors (i.e., oscillations in the solution), as described by Crank (1975) and other authors. Landscape evolution is calculated by updating the topography at the end of each time step. Similarly, conservation of mass is checked after each time step by summing elevation values for each cell across the topographic grid.

Only minimal information about redistribution can be obtained from the remaining traces of tephra in the Yucca Mountain area, and data derived from analog areas lack a comparable climate and volcanological character. Lathrop Wells is the youngest scoria cone volcano in the Yucca Mountain region of southern Nevada. Almost the entire 80,000-year-old (Heizler, et al., 1999) tephra deposit has been eroded away, but the initial volume has been estimated to be 0.04 km^3 [0.0096 mi^3] based on cone:fall volume-ratios at analog volcanoes (Bechtel SAIC Company, LLC., 2003c,d; NRC, 1999). Despite the limited availability of preserved primary tephra, Bechtel SAIC Company, LLC. (2003c,d) put forth an isopach map. The isopachs are admittedly conjectural, but from this study the estimated area encompassed by the 1-cm [0.4-in] isopach is 182 km^2 [70.3 mi^2] with an estimated deposit perimeter of 50 km [31 mi]. The length of time required to erode the majority of the Lathrop Wells tephra deposit, meaning roughly to the present degree of erosion, was calculated at 29,000 years[1] (Hooper and Hill, 2004). This time was based on a first-order conceptual model in which the sediment yield increases 1–7 times in the first 30 years after an eruption (i.e., based on Parícutin volcano, Mexico) (Hooper, 2004). For these calculations in the first-order model, sediment yield was 15 $m^3\ km^{-2}\ yr^{-1}$ [1,372 $ft^3\ mi^{-2}\ yr^{-1}$], and tephra dilution through mixing with other sediment was 50 percent.

Using the parameters for Lathrop Wells, the volumetric transport rate (or discharge), Q_{LW}, can be calculated by

$$Q_{LW} = \frac{(V_t + V_s)}{t} = 2.8 \times 10^3\ \mathrm{m^3/yr} \tag{4-5}$$

where V_t is the volume of tephra {$4 \times 10^7\ m^3$ [1.4×10^9 ft3]}, V_s is the volume of non-volcanic sediment (assuming 50 percent dilution, $V_t = V_s$), and t is the estimated time (29,000 years) to erode the initial Lathrop Wells deposit. The diffusion coefficient, D_{LW}, is calculated by dividing the volumetric transport rate by the perimeter or erosional front of the deposit, x_p:

$$D_{LW} = \frac{Q_{LW}}{x_p} = 5.5 \times 10^{-2}\ \mathrm{m^2/yr} \tag{4-6}$$

where x_p is 50,000 m [164,040 ft].

[1]Hooper, D.M. “Volcanological Investigations.” Scientific Notebook 662E. San Antonio, Texas: CNWRA.

The volumetric transport rate per unit slope width for unaffected slopes in the same drainage basin is

$$Q_{\text{norm}} = Y_{LW} \times A_{LW} = 5.0\,\text{m}^3\,\text{km}^{-2}\,\text{yr}^{-1} \times 182\ \text{km}^2 = 910\ \text{m}^3\,\text{yr}^{-1} \tag{4-7}$$

where A_{LW} is the estimated area {182 km^2 [70.3 mi^2]} encompassed by the 1-cm [0.4-in] isopach, and Y_{LW} is estimated sediment yield for the basin that drains Lathrop Wells, adjacent to Fortymile Wash. This value was selected to be approximately the same as Y_{sed}, the sediment yield for Fortymile Wash (Table 3-1). Q_{norm} also can be considered the ambient or preeruption flux. The diffusion coefficient, D_{norm}, is calculated by dividing the volumetric transport rate by the same perimeter or erosional front for the deposit, x_p:

$$D_{\text{norm}} = \frac{Q_{\text{norm}}}{x_p} = 1.8 \times 10^{-2}\,\text{m}^2\,\text{yr}^{-1} \tag{4-8}$$

The simulation grid was devised to represent the natural landscape of the Fortymile Wash catchment basin. Grid cells with zero slope added to create the depositional basin form an easily recognizable knickpoint, or change in slope, with the rest of the topography (Figure 4-3), similar to what is encountered as Fortymile Wash becomes an unconfined depositional (or aggrading) fan in the vicinity of U.S. Highway 95. This point serves as an artificial stream gage for measuring sediment discharge rather than stream discharge. Total mass transported per time step can be calculated by multiplying the amount of aggrading material in the grid cell by unit cell size, which is 30 m [98.4 ft]. Initially, the sediment discharge is just the contribution from the adjacent cell, but as time passes the sediment flux increases as the contribution from more distant cells reaches the knickpoint, just as it would in a natural setting. This process is identical to what was observed by Segerstrom (1961) and Inbar, et al. (1994) for the erosion of the Parícutin tephra deposit (Figure 4-1): sediment yield increases rapidly, peaks, and then gradually declines. To quantitatively describe this result, D_{norm} is a measure of ambient sediment transport, while D_{LW} is a measure of accelerated erosion. The initial difference in sediment transport is related to the ratio

$$\frac{D_{LW}}{D_{\text{norm}}} = 3 \tag{4-9}$$

To compute the relative sediment yield, D_{norm} and the ambient sediment yield remain constant, but sediment transport measured as part of the eroding tephra deposit increases because of the higher diffusion coefficient. Thus, the relative sediment yield calculated by this procedure has an initial value of 3 times the preeruption sediment yield in the first year after the deposition of the tephra (or the first year with a flood event for the case of ephemeral streams). Accelerated erosion elevates the sediment yield to 4.6 times the preeruption yield after 490 years before slowly returning to the normal rate as tephra depletion is simulated by redistributed material and a reduction in slope angle. Results are illustrated in Figure 4-4.

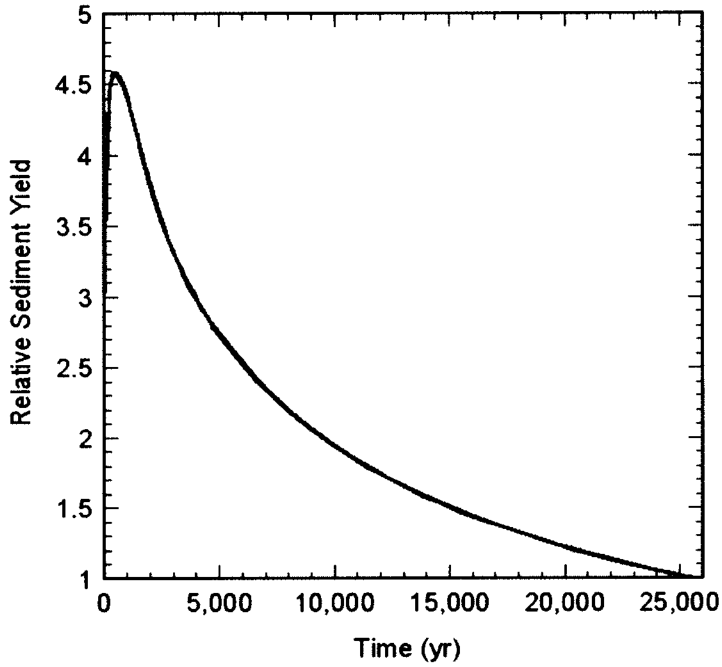

Figure 4-4. Plot of Calculated Accelerated Erosion Following Potential Tephra Fall in the Fortymile Wash Drainage System. In the Aftermath of an Eruption, There is an Increase in Sediment Yield (Accelerated Erosion) and Then a Gradual Decrease in Sediment Yield from These Elevated Values Until Conditions Return to the Preeruption Yield {Which is a Relative Sediment Yield of 1.0 [unitless]}.

5 REDISTRIBUTION MODELING RESULTS

5.1 Results

All parameters for the Fortymile Wash sediment budget have now been defined, including sediment yield and mass of tephra potentially deposited within the catchment basin. In order to abstract a redistribution model that is useable in TPA code calculations, all erosion is lumped into a single annual term, the sediment yield, rather than modeling the separate contributions from individual hillslope processes. Dilution is the ratio of eroded tephra to total sediment in the Fortymile Wash depositional fan. Redistribution model parameters and components are described in Table 5-1, and Figure 5-1 illustrates the conceptual framework. The redistribution model is outlined as follows:

(1) The appropriate relative sediment yield value is assigned based on the age of the deposit. Under ambient or normal conditions the relative sediment yield has a value of 1.0. Accelerated erosion changes through time and follows Figure 4-4.

(2) The mass of eroded tephra is determined by multiplying annual erosion rate by the mass and area affected by tephra deposition. Each mathematical expression is listed in Table 5-1.

(3) The mass of eroded tephra that reaches the Fortymile Wash depositional fan (i.e., the basin outlet) is summed.

(4) The mass of ambient sediment (i.e., non-tephra material) that reaches the Fortymile Wash depositional fan is summed.

(5) The total mass of ambient sediment and eroded tephra in the depositional fan is calculated.

(6) Tephra dilution, expressed as a percentage, is calculated.

(7) The mass of tephra remaining in the Fortymile Wash catchment basin is calculated.

(8) The percentage of tephra remaining in the Fortymile Wash catchment basin is calculated.

Two key parameters, sediment yield (Y_{sed}) and mass of erupted tephra ($M_{teph,erup}$), were evaluated within the sediment budget to help model uncertainty and estimate risk. The sediment budget or tephra redistribution model was run with these terms set to fixed values. To capture the spread of data around the mean, the ±2 standard deviation values also were used (Table 3-1). Approximately 95 percent of all observations are included within this interval. Therefore, 9 sediment budget scenarios or cases were run. The high sediment yield value (+2σ) indicates a higher rate of sediment transport to the Fortymile Wash depositional fan or basin than the “low” sediment yield value (−2σ) with a slower erosion rate. The mass of erupted tephra is also set at mean, high (+2σ), and low (−2σ) values depending on the amount of erupted tephra calculated from 1,024 realizations of the TEPHRA code (Table 3-1). Another parameter, A_{teph} (area of Fortymile Wash catchment basin covered by tephra), was not varied but treated as a constant for

Table 5-1. Sediment Budget Parameters		
Parameter Name	**Description**	**Value**
T	Time increment [yr]	set by user
A_{fmw}	Area of Fortymile Wash Catchment Basin	815 km^2
A_{teph}	Area of Fortymile Wash Catchment Basin Covered by Tephra	149 km^2
a_{teph}	Areal Fraction of Fortymile Wash Catchment Basin Covered by Tephra	149/815 = 0.183
a_{amb}	Areal Fraction of Fortymile Wash Catchment Basin not Covered by Tephra (Considered the Ambient or Unaffected Portion of the Basin)	666/815 = 0.817
Y_{rel}	Relative Sediment Yield [Unitless]	1.0 to 4.6 (Sampled Parameter from Figure 4-4)
Y_{sed}	Sediment Yield (a Measure of Sediment Transport to the Fortymile Wash Depositional Fan)	8.9×10^6 kg/yr (Mean) 1.5×10^7 kg/yr (+2σ) 2.9×10^6 kg/yr (−2σ)
Y_{teph}	Sediment Yield Derived from the Tephra-Covered Portion of the Fortymile Wash Catchment Basin [kg/yr]	$Y_{teph} = Y_{sed} \times Y_{rel} \times a_{teph} \times T$
$M_{teph,erup}$	Mass of Erupted Tephra in the Fortymile Wash Catchment Basin	2.5×10^{10} kg (Mean) 8.1×10^{10} kg (+2σ) 6.9×10^9 kg (−2σ)
$M_{teph,fan}$	Mass of Tephra in the Fortymile Wash Depositional Fan [kg]	$M_{teph,fan} = \sum Y_{teph}$
$M_{sed,fan}$	Mass of Ambient Sediment in the Fortymile Wash Depositional Fan [kg]	$M_{sed,fan} = Y_{sed} \times Y_{rel} \times a_{amb} \times T$; where $Y_{rel} = 1$
$M_{tot,fan}$	Total tephra and Sediment in the Fortymile Wash Depositional Fan [kg]	$M_{tot,fan} = M_{teph,fan} + M_{sed,fan}$
Dilution	Ratio of Eroded Tephra to Total Sediment Transported to the Fortymile Wash Depositional Fan	$(M_{teph,fan}/M_{tot,fan}) \times 100$
$M_{teph,rem}$	Mass of Tephra Remaining in the Fortymile Wash Catchment Basin [kg]	$M_{teph,rem} = M_{teph,erup} - M_{teph,fan}$
$M_{rem,per}$	Mass of Tephra Remaining in the Fortymile Wash Catchment Basin (Expressed as a Percentage)	$M_{rem,per} = (M_{teph,rem}/M_{teph,erup}) \times 100$

these sediment budget runs. Each sediment budget was stopped when the tephra was 100 percent depleted, which is similar to the present condition at Lathrop Wells, so that tephra depletion is the length of time in years to completely remove or exhaust the tephra originally deposited in the catchment basin of Fortymile Wash. The sediment budget is run in a spreadsheet, and selected time steps for all nine cases are recorded in Hooper[1]. Table 5-2

[1]Hooper, D.M. "Volcanological Investigations." Scientific Notebook 662E. San Antonio, Texas: CNWRA.

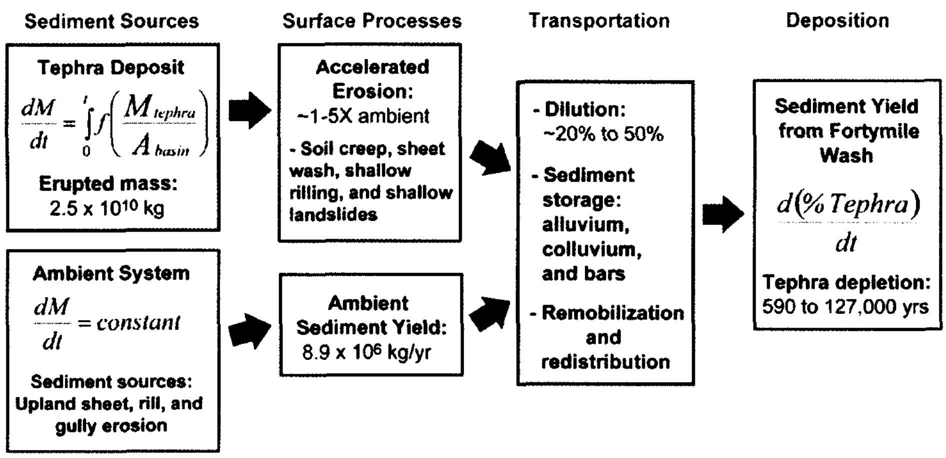

Figure 5-1. Overview of the Sediment Budget for Fortymile Wash Following a Potential Tephra-Fall Deposit

illustrates Case 5, the sediment budget for mean values of sediment yield and mass of erupted tephra. For brevity, the entire output is not listed in this table and the time increment (year) changes from every 4 years at the beginning to every 200 years by the end of the table. Table 5-2 contains more decimal places than justified by significant figures. This is a carry-over from error-detection with a large number of time steps and mass-balance checks. By employing the statistical means for key parameters (Case 5, Table 5-2), approximately 98 percent of the tephra deposit remains in the Fortymile Wash catchment basin after 100 years and approximately 72 percent of the tephra deposit remains after 1,000 years. Table 5-3 summarizes the results of the sediment budget calculations for Fortymile Wash.

Table 5-3 reveals several important trends and outcomes. As anticipated, the case of a high sediment yield rate acting upon a small-volume deposit (Case 1) depletes the tephra rapidly in 590 years. Conversely, the case of a low sediment yield rate acting upon a large-volume deposit (Case 9) depletes the tephra slowly in 127,000 years. Using the mean values for sediment yield and mass of erupted tephra (Case 5) produces a result of 4,100 years for tephra depletion. Figure 5-2 illustrates the mass of tephra reaching the Fortymile Wash depositional fan (i.e., the approximate site of the reasonably maximally exposed individual) over time for Case 5.

Dilution, the ratio of eroded tephra to total sediment, mostly ranges between 40 and 50 percent in these calculations (Table 5-3 and Figure 5-3). The maximum dilution value of 49.4 percent is a function of modeled accelerated erosion, as well as the fixed basin area covered by tephra. The longer it takes to deplete the tephra deposit, the greater the opportunity for tephra to be mixed with ambient sediment. This is demonstrated by the two longest model runs, Cases 6 and 9. Requiring 24,500 years to deplete the tephra deposit, fan deposits in Case 6 are 31.3 percent tephra; whereas deposits for Case 9 are 21.1 percent tephra after 127,000 years. Case 1, with high sediment yield and a low erupted mass, only achieves a maximum dilution in the fan deposit of 48.8 percent because the tephra is depleted so rapidly (in 590 years).

Table 5-2. Fortymile Wash Sediment Budget (Case 5: Y_{sed} = mean, $M_{teph,erup}$ = mean)

Year	Y_{rel}	Y_{teph} (kg)	$M_{teph,fan}$ (kg)	$M_{sed,fan}$ (kg)	$M_{tot,fan}$ (kg)	Dilution (%)	$M_{teph,rem}$ (kg)	$M_{rem,per}$ (%)
4	3.036	1.9779×10^{7}	1.9779×10^{7}	2.9085×10^{7}	4.8864×10^{7}	40.48	2.498×10^{10}	99.92
8	3.051	1.9877×10^{7}	3.9655×10^{7}	5.817×10^{7}	9.7826×10^{7}	40.54	2.496×10^{10}	99.84
12	3.066	1.9974×10^{7}	5.963×10^{7}	8.7256×10^{7}	1.4689×10^{8}	40.6	2.494×10^{10}	99.76
16	3.081	2.0072×10^{7}	7.9702×10^{7}	1.1634×10^{8}	1.9604×10^{8}	40.66	2.492×10^{10}	99.68
20	3.097	2.0176×10^{7}	9.9878×10^{7}	1.4543×10^{8}	2.453×10^{8}	40.72	2.49×10^{10}	99.6
24	3.135	2.0424×10^{7}	1.203×10^{8}	1.7451×10^{8}	2.9481×10^{8}	40.81	2.488×10^{10}	99.52
28	3.173	2.0671×10^{7}	1.4097×10^{8}	2.036×10^{8}	3.4457×10^{8}	40.91	2.4859×10^{10}	99.44
32	3.211	2.0919×10^{7}	1.6189×10^{8}	2.3268×10^{8}	3.9457×10^{8}	41.03	2.4838×10^{10}	99.35
36	3.249	2.1167×10^{7}	1.8306×10^{8}	2.6177×10^{8}	4.4483×10^{8}	41.15	2.4817×10^{10}	99.27
40	3.287	2.1414×10^{7}	2.0447×10^{8}	2.9085×10^{8}	4.9533×10^{8}	41.28	2.4796×10^{10}	99.18
44	3.325	2.1662×10^{7}	2.2614×10^{8}	3.1994×10^{8}	5.4607×10^{8}	41.41	2.4774×10^{10}	99.1
48	3.363	2.1909×10^{7}	2.4804×10^{8}	3.4902×10^{8}	5.9707×10^{8}	41.54	2.4752×10^{10}	99.01
52	3.401	2.2157×10^{7}	2.702×10^{8}	3.7811×10^{8}	6.4831×10^{8}	41.68	2.473×10^{10}	98.92
56	3.439	2.2404×10^{7}	2.9261×10^{8}	4.0719×10^{8}	6.998×10^{8}	41.81	2.4707×10^{10}	98.83
60	3.477	2.2652×10^{7}	3.1526×10^{8}	4.3628×10^{8}	7.5154×10^{8}	41.95	2.4685×10^{10}	98.74
80	3.667	2.389×10^{7}	4.3223×10^{8}	5.817×10^{8}	1.0139×10^{9}	42.63	2.4568×10^{10}	98.27
100	3.813	2.484×10^{7}	5.5482×10^{8}	7.2713×10^{8}	1.2819×10^{9}	43.28	2.4445×10^{10}	97.78
200	4.269	2.7815×10^{7}	1.2222×10^{9}	1.4543×10^{9}	2.6765×10^{9}	45.67	2.3778×10^{10}	95.11
300	4.485	2.9222×10^{7}	1.9398×10^{9}	2.1814×10^{9}	4.1212×10^{9}	47.07	2.306×10^{10}	92.24
400	4.569	2.9766×10^{7}	2.6795×10^{9}	2.9085×10^{9}	5.588×10^{9}	47.95	2.232×10^{10}	89.28
600	4.567	2.9753×10^{7}	4.17×10^{9}	4.3628×10^{9}	8.5328×10^{9}	48.87	2.083×10^{10}	83.32
800	4.493	2.9271×10^{7}	5.6473×10^{9}	5.817×10^{9}	1.1464×10^{10}	49.26	1.9353×10^{10}	77.41
1,000	4.4	2.8665×10^{7}	7.0955×10^{9}	7.2713×10^{9}	1.4367×10^{10}	49.39	1.7905×10^{10}	71.62
1,200	4.288	1.3968×10^{8}	8.5099×10^{9}	8.7256×10^{9}	1.7235×10^{10}	49.37	1.649×10^{10}	65.96
1,400	4.164	1.3564×10^{8}	9.8852×10^{9}	1.018×10^{10}	2.0065×10^{10}	49.27	1.5115×10^{10}	60.46
1,600	4.036	1.3147×10^{8}	1.1219×10^{10}	1.1634×10^{10}	2.2853×10^{10}	49.09	1.3781×10^{10}	55.13
1,800	3.912	1.2743×10^{8}	1.2511×10^{10}	1.3088×10^{10}	2.5599×10^{10}	48.87	1.2489×10^{10}	49.96
2,000	3.791	1.2349×10^{8}	1.3763×10^{10}	1.4543×10^{10}	2.8306×10^{10}	48.62	1.1237×10^{10}	44.95
2,200	3.685	6.0018×10^{8}	1.4972×10^{10}	1.5997×10^{10}	3.0969×10^{10}	48.35	1.0028×10^{10}	40.11

5-4

Table 5-2. Fortymile Wash Sediment Budget (Case 5: Y_{sed} = mean, $M_{teph,erup}$ = mean) (continued)								
Year	**Y_{rel}**	**Y_{teph} (kg)**	**$M_{teph,fan}$ (kg)**	**$M_{sed,fan}$ (kg)**	**$M_{tot,fan}$ (kg)**	**Dilution (%)**	**$M_{teph,rem}$ (kg)**	**$M_{rem,per}$ (%)**
2,400	3.579	5.8291×10^{8}	1.6147×10^{10}	1.7451×10^{10}	3.3598×10^{10}	48.06	8.8534×10^{9}	35.41
2,600	3.485	5.676×10^{8}	1.7288×10^{10}	1.8905×10^{10}	3.6194×10^{10}	47.77	7.7116×10^{9}	30.85
2,800	3.405	5.5457×10^{8}	1.8404×10^{10}	2.036×10^{10}	3.8764×10^{10}	47.48	6.596×10^{9}	26.38
3,000	3.326	5.4171×10^{8}	1.9494×10^{10}	2.1814×10^{10}	4.1308×10^{10}	47.19	5.5062×10^{9}	22.02
3,200	3.246	5.2868×10^{8}	2.0558×10^{10}	2.3268×10^{10}	4.3826×10^{10}	46.91	4.4424×10^{9}	17.77
3,400	3.166	5.1565×10^{8}	2.1595×10^{10}	2.4722×10^{10}	4.6318×10^{10}	46.62	3.4045×10^{9}	13.62
3,600	3.107	5.0604×10^{8}	2.2611×10^{10}	2.6177×10^{10}	4.8787×10^{10}	46.35	2.3894×10^{9}	9.56
3,800	3.051	4.9692×10^{8}	2.3609×10^{10}	2.7631×10^{10}	5.124×10^{10}	46.08	1.391×10^{9}	5.56
4,000	2.996	4.8796×10^{8}	2.4589×10^{10}	2.9085×10^{10}	5.3675×10^{10}	45.81	4.1067×10^{8}	1.64
4,100	2.968	4.834×10^{8}	2.5073×10^{10}	2.9812×10^{10}	5.4885×10^{10}	45.68	-7.273×10^{7}	−0.29

Table 5-3. Tephra Redistribution Modeling Results

		Mass of Erupted Tephra ($M_{teph,erup}$)		
		Low (−2σ)	Mean ($\bar{x}$)	High (+2σ)
Sediment Yield (Y_{sed})	High (+2σ)	**Case 1** Tephra depletion: 590 years Dilution: 40.5–48.8 %	**Case 2** Tephra depletion: 2,200 years Dilution: 40.5–49.4%	**Case 3** Tephra depletion: 10,000 years Dilution: 39.6–49.4%
	Mean ($\bar{x}$)	**Case 4** Tephra depletion: 972 years Dilution: 40.5–49.4%	**Case 5** Tephra depletion: 4,100 years Dilution: 40.5–49.4%	**Case 6** Tephra depletion: 24,500 years Dilution: 31.3–49.4%
	Low (-2σ)	**Case 7** Tephra depletion: 3,300 years Dilution: 40.5–49.4%	**Case 8** Tephra depletion: 22,000 years Dilution: 32.4–49.4%	**Case 9** Tephra depletion: 127,000 years Dilution: 21.1–49.4%

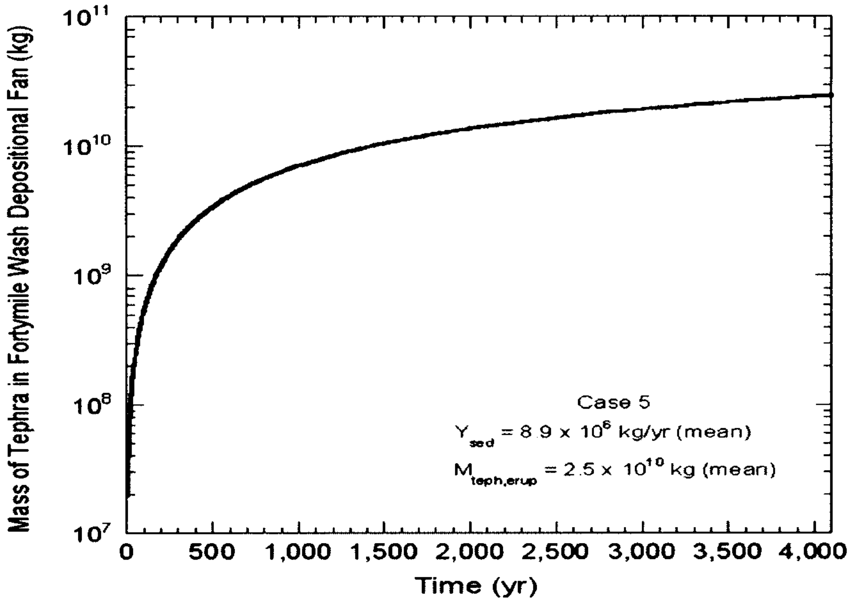

Figure 5-2. Plot of Mass of Tephra at the Fortymile Wash Depositional Fan Versus Time. Case 5 is Shown for Mean Sediment Yield (Y_{sed}), Mean Mass of Erupted Tephra ($M_{teph,erup}$), and Tephra Depletion After 4,100 Years.

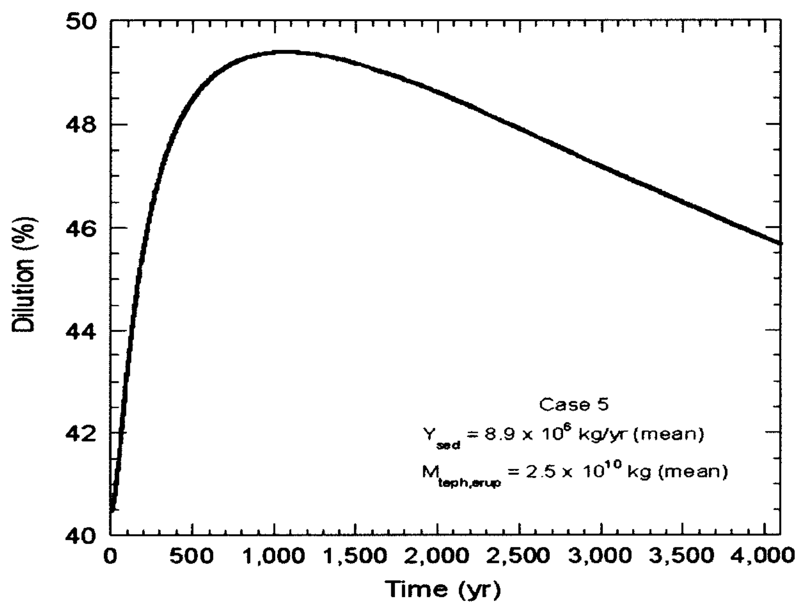

Figure 5-3. Plot of Dilution of Tephra at the Fortymile Wash Depositional Fan Versus Time. Case 5 is Shown for Mean Sediment Yield (Y_{sed}), Mean Mass of Erupted Tephra ($M_{teph,erup}$), and Tephra Depletion After 4,100 Years. Dilution is the Ratio of Eroded Tephra to Total Sediment in the Fortymile Wash Depositional Fan or Basin.

6 SUMMARY AND CONCLUSIONS

This report describes a simplified process-level model that has been developed to evaluate the long-term fluvial redistribution of tephra in Fortymile Wash at Yucca Mountain, Nevada. A violent-strombolian eruption producing a basaltic tephra-fall deposit could disrupt the supply of sediment to rivers and trigger accelerated erosion. In the aftermath of the volcanic eruption, the magnitude and duration of this perturbation to the sediment yield depends upon climatic setting, terrain, and nature of the erupted material. In the event of a volcanic eruption through the potential repository at Yucca Mountain, high-level waste also may be transported in the volcanic plume, with the potential deposition of radionuclides at the reasonably maximally exposed individual (or receptor) location, either from direct sedimentation from the volcanic tephra cloud or from the remobilization of tephra by water (i.e., Fortymile Wash) and wind after initial deposition.

Fortymile Wash, an ephemeral stream, is the primary drainage for Yucca Mountain. Hydrologic data, however, are minimal, and sediment transport data are lacking. Rates of erosion in arid regions are not well-constrained, but a suitable range of values can be entered into the sediment budget model to demonstrate the quantitative or mass flux relationship between such components as sediment yield, dilution by mixing with ambient sediment, balance of remaining tephra, associated changes in sediment storage, and discharge to the depositional fan as a function of time after the eruption. To the greatest extent possible, analyses consider appropriate uncertainties in data and address site-specific processes. Hillslope processes are largely simplified because soil properties and slope characteristics for tephra-covered hillsides in an arid region are unknown.

For the tephra redistribution case that applies statistical means for key parameters, the percentage of the Fortymile Wash catchment basin that is covered by tephra is 18 percent. Model results utilizing mean values for sediment yield and mass of erupted tephra reveal that tephra depletion in the Fortymile Wash catchment basin requires 4,100 years and the ratio of eroded tephra to total sediment transported to the Fortymile Wash depositional basin (i.e., dilution) ranges from 40 to 50 percent. This suggests that potential basaltic tephra deposits within Fortymile Wash are not rapidly diluted within a few hundred years of deposition and that their erosion cannot be explained well by a simple decay relationship. Therefore, the posteruption redistribution of tephra is potentially risk significant as remobilized tephra deposits may affect airborne particle concentrations and their persistence for the reasonably maximally exposed individual.

Remobilization of ash (i.e., tephra) deposits has medium significance to waste isolation (NRC, 2004). This report communicates the current understanding of tephra redistribution analyses independently developed by CNWRA staff. Findings from these analyses are expected to assist in preparing for review of a license application for a potential repository at Yucca Mountain, Nevada. Insights gained from this report will help staff prepare a technical basis to review DOE models that address remobilization and redistribution.

7 REFERENCES

Amos, R.C. "Sunset Crater, Arizona: Evidence for a Large Magnitude Strombolian Eruption." Master thesis. Arizona State University. Tempe, Arizona. 1986.

Anderson, R.S. "Evolution of the Santa Cruz Mountains, California, through Tectonic Growth and Geomorphic Decay." *Journal of Geophysical Research*. Vol. 99. No. B10. pp. 20,161–20,179. 1994.

Andrews, D.J. and R.C. Bucknam. "Fitting Degradation of Shoreline Scarps by a Nonlinear Diffusion Model." *Journal of Geophysical Research*. Vol. 92. pp. 12,857–12,867. 1987.

Andrews, D.J. and T.C. Hanks. "Scarp Degraded by Linear Diffusion: Inverse Solution for Age." *Journal of Geophysical Research*. Vol. 90. pp. 10,193–10,208. 1985.

Bechtel SAIC Company, LLC. "Atmospheric Dispersal and Deposition of Tephra from a Potential Volcanic Eruption at Yucca Mountain, Nevada." MDL–MGR–GS–000002. Rev. 00. Las Vegas, Nevada: Bechtel SAIC Company, LLC. 2004.

———. "Characteristics of the Receptor for the Biosphere Model." ANL–MGR–MD–000005. Rev. 2. Las Vegas, Nevada: Bechtel SAIC Company, LLC. 2003a.

———. "Inhalation Exposure Input Parameters for the Biosphere Model." ANL–MGR–MD–000001. Rev. 2 ICN 0. Las Vegas, Nevada: Bechtel SAIC Company, LLC. 2003b.

———. "Characterize Eruptive Processes at Yucca Mountain, Nevada." ANL–MGR–GS–000002. Rev.1. Las Vegas, Nevada: Bechtel SAIC Company, LLC. 2003c.

———. "Technical Basis Document No. 13: Volcanic Events." Rev. 2. Las Vegas, Nevada: Bechtel SAIC Company, LLC. 2003d.

Beck, D.A. and P.A. Glancy. "Overview of Runoff of March 11, 1995, in Fortymile Wash and Amargosa River, Southern Nevada." U.S. Geological Survey Fact Sheet FS–210–95. 1995.

Benke, R., D. Hooper, B. Hill, R. Nes, and B. Winfrey. "Chapter 6: Ash Remobilization Modeling for Extrusive Volcanism." Risk Analysis for Risk Insight Progress Report. San Antonio, Texas: CNWRA. 2005.

Bull, L.J. and M.J. Kirkby (eds.). "Dryland Rivers: Hydrology and Geomorphology of Semi-Arid Channels." United Kingdom: John Wiley & Sons. 2002.

Bullard, K.L. "Nevada Test Site Probable Maximum Flood Study, Part of U.S. Geological Survey Flood Potential and Debris Hazard Study, Yucca Mountain Site." Denver, Colorado: U.S. Department of the Interior, Bureau of Reclamation. 1992.

Carslaw, H.S. and J.C. Jaeger. "Conduction of Heat in Solids." (2nd. ed.). London, United Kingdom: Oxford University Press. p. 510. 1959.

Carson, M.A. and M.J. Kirkby. "Hillslope Form and Process." London, United Kingdom: Cambridge University Press. p. 475. 1972.

Cas, R.A.F. and J.V. Wright. "Volcanic Successions, Modern and Ancient." London, United Kingdom: Allen & Unwin. p. 528. 1987.

Chinen, T. and H. Kadomura. "Post-Eruption Sediment Budget of a Small Catchment on Mt. Usu, Hokkaido." *Zeitschrift für Geomorphologie*. Suppl.-Bd. 60. pp. 217–232. 1986.

Coe, J.A, P.A. Glancy, and J.W. Whitney. "Volumetric Analysis and Hydrologic Characterization of a Modern Debris Flow Near Yucca Mountain, Nevada." *Geomorphology.* Vol. 20. pp. 11–28. 1997.

Collins, B.D. and T. Dunne. "Erosion of Tephra from the 1980 Eruption of Mount St. Helens." *Geological Society of America Bulletin*. Vol. 97. pp. 896–905. 1986.

Collins, B.D., T. Dunne, and A.K. Lehre. "Erosion of Tephra-Covered Hillslopes North of Mount St. Helens, Washington: May 1980–May 1981." *Zeitschrift für Geomorphologie*. Suppl.-Bd. 46. pp. 103–121. 1983.

Colman, S.M. and K. Watson. "Ages Estimated From a Diffusion Equation Model for Scarp Degradation." *Science*. Vol. 221. pp. 263–265. 1983.

Costa, J.E. and V.R. Baker. "Surficial Geology, Building with the Earth." New York City, New York: John Wiley & Sons. 1981.

Crank, J. "The Mathematics of Diffusion." (2nd. ed.). London, United Kingdom: Oxford University Press. p. 414. 1975.

CRWMS M&O. "Yucca Mountain Site Description Document." Section 7—Surface Water Hydrology. TDR–CRW–GS–000001. Rev. 01 ICN 01. Las Vegas, Nevada: CRWMS M&O. 2000.

Culling, W.E.H. "Analytical Theory of Erosion." *Journal of Geology*. Vol. 68. pp. 336–344. 1960.

———. "Soil Creep and the Development of Hillside Slopes." *Journal of Geology*. Vol. 71. pp. 127–161. 1963.

———. "Theory of Erosion on Soil-Covered Slopes." *Journal of Geology*. Vol. 73. pp. 230–254. 1965.

Dietrich, W.E. and T. Dunne. "Sediment Budget for a Small Catchment in Mountainous Terrain." *Zeitschrift für Geomorphologie*. Suppl.-Bd 29. pp. 191–206. 1978.

Dietrich, W.E., T. Dunne, N.F. Humphrey, and L.M. Reid. "Construction of Sediment Budgets for Drainage Basins." *Sediment Budgets and Routing in Forested Drainage Basins*. General Technical Report PNW–141. Portland, Oregon: U.S. Department of Agriculture, Forest Service, Pacific Northwest Forest and Range Experiment Station. pp. 5–23. 1982.

DOE. "Evaluation of the Potentially Adverse Condition Evidence of Extreme Erosion During the Quaternary Period at Yucca Mountain, Nevada." YMP/92–41–TPR. North Las Vegas, Nevada: DOE, Yucca Mountain Site Characterization Office. 1993.

Glancy, P.A. "Evidence of Prehistoric Flooding and the Potential for Future Extreme Flooding at Coyote Wash, Yucca Mountain, Nye County, Nevada." U.S. Geological Survey Open-File Report 92–458. p.31. 1994.

Glancy, P.A. and D.A. Beck. "Modern Flooding and Runoff of the Amargosa River, Nevada–California, Emphasizing Contributions of Fortymile Wash." Quaternary Geology of the Yucca Mountain Area, Southern Nevada. Field Trip Guide. E.M. Taylor, ed. 1998 Annual Meeting of the Friends of the Pleistocene, Pacific Cell. 1998.

Graf, W.H. "Hydraulics of Sediment Transport." New York City, New York: McGraw-Hill. 1971.

Graf, W.L. "Fluvial Processes in Dryland Rivers." (Caldwell, New Jersey: The Blackburn Press. 2002 reprinted edition). Berlin: Springer-Verlag. 1988.

Gringorten, I.I. "A Plotting Rule for Extreme Probability Paper." *Journal of Geophysical Research*. Vol. 68. No. 3. pp. 813–814. 1963.

Hanks, T.C., R.C. Bucknam, K.R. Lajoie, and R.E. Wallace. "Modification of Wave-Cut and Faulting-Controlled Landforms." *Journal of Geophysical Research*. Vol. 89. pp. 5771–5790. 1984.

Hanks, T.C. and R.E. Wallace. "Morphological Analysis of the Lake Lahontan Shoreline and Beachfront Fault Scarps, Pershing County, Nevada." *Bulletin of the Seismological Society of America*. Vol. 75. No. 3. pp. 835–846. 1985.

Harbaugh, J.W. and G. Bonham-Carter. "Computer Simulation in Geology." New York, New York: John Wiley & Sons. p. 575. 1970.

Heizler, M.T., F.V. Perry, B.M. Crowe, L. Peters, and R. Appelt. "The Age of Lathrop Wells Volcanic Center: An $^{40}Ar/^{39}Ar$ Dating Investigation." *Journal of Geophysical Research*. Vol. 104 (B1). pp. 767–804. Washington, DC: American Geophysical Union. 1999.

Hill, B.E. and C.B. Connor. "Technical Basis for Resolution of the Igneous Activity Key Technical Issue." San Antonio, Texas: CNWRA. 2000.

Hill, B.E., C.B. Connor, M.S. Jarzemba, P.C. La Femina, M. Navarro, and W. Strauch. "1995 Eruptions of Cerro Negro Volcano, Nicaragua, and Risk Assessment for Future Eruptions. *Geological Society of America Bulletin*. Vol. 10. pp. 1,231–1,241. 1998.

Holm, R.F. and R.B. Moore. "Holocene Scoria Cone and Lava Flows at Sunset Crater, Northern Arizona." Geological Society of America Centennial Field Guide–Rocky Mountain Section. Vol. 2. DNAG Project. pp. 393–397. 1987.

Hooper, D.M. "First-Order Conceptual Model for Fluvial Remobilization of Tephra Along Fortymile Wash, Yucca Mountain, Nevada." San Antonio, Texas: CNWRA. 2004.

Hooper, D.M. and B.E. Hill. “Geomorphic Evolution of the Tephra Deposit From Paricutin Volcano, Mexico.” Poster presented at the International Association of Volcanology and Chemistry of the Earth Interior General Assembly, Pucón, Chile. Doc # (ELF): Q200410180002. October 4, 2004. San Antonio, Texas: CNWRA. 2004.

Inbar, M., J.L Hubp, and L.V. Ruiz. “The Geomorphological Evolution of the Parícutin Cone and Lava Flows, Mexico, 1943–1990.” *Geomorphology*. Vol. 9. pp. 57–76. 1994.

Jarzemba, M.S., P.A. LaPlante, and K.J. Poor. “ASHPLUME Version 1.0—A Code for Contaminated Ash Dispersal and Deposition.” CNWRA 97-004. San Antonio, Texas: CNWRA. 1997.

Julien, P.Y. “Erosion and Sedimentation.” Cambridge, United Kingdom: Cambridge University Press. 1998.

Kadomura, H., T. Imagawa, and H. Yamamoto. “Eruption-Induced Rapid Erosion and Mass Movements on Usu Volcano, Hokkaido.” *Zeitschrift für Geomorphologie*. Suppl.-Bd. 46. pp. 123–142. 1983.

Kane, T.G., D.J. Bauer, and C.M. Martinez. “Streamflow and Selected Precipitation Data for Yucca Mountain Region, Southern Nevada and Eastern California, Water Years 1986–90.” U.S. Geological Survey Open-File Report 94–312. p. 118. 1994.

Kirkby, M.J. “Hillslope Process-Response Models Based on the Continuity Equation.” Institute of British Geographers Special Publication. Vol. 3. pp. 15–30. 1971.

Knighton, D. “Fluvial Forms and Processes.” London, United Kingdom: Arnold Publishers. p. 383. 1998.

Kokajko, L.E. “Staff Review of U.S. Department of Energy Response to Igneous Activity Agreement Item IA.2.17.” Letter with Enclosures (January 10) to J.D. Ziegler, DOE. Washington, DC: NRC. 2005.

Komar, P.D. “Sediment Transport by Floods.” *Flood Geomorphology*. New York City, New York: John Wiley & Sons/A Wiley-Interscience Publication. pp. 97–111. 1988.

Kooi, H. and C. Beaumont. “Escarpment Evolution on High-Elevation Rifted Margins: Insights Derived from a Surface Processes Model That Combines Diffusion, Advection, and Reaction.” *Journal of Geophysical Research*. Vol. 99. No. B6. pp. 12,191–12,209. 1994.

Laronne, J.B. and I. Reid. “Very High Rates of Bedload Sediment Transport by Ephemeral Desert Rivers.” *Nature*. Vol. 366. p. 148–150. 1993.

Lehre, A.K. “Sediment Budget of a Small Coast Range Drainage Basin in North-Central California.” Sedment Budgets and Routing in Forested Drainage Basins. General Technical Rep[ort PNW–141. Portland, Oregon: U.S. Department of Agriculture, Forest Service, Pacific Northwest Forest and Range Experiment Station. pp. 67–77. 1982.

Lehre, A.K., B.D. Collins, and T. Dunne. "Post-Eruption Sediment Budget for the North Fork Toutle River Drainage, June 1980–June 1981." *Zeitschrift für Geomorphologie*. Suppl.-Bd. 46. pp. 143–163. 1983.

Leopold, L.B., M.G. Wolman, and J.P. Miller. "Fluvial Processes in Geomorphology." (New York City, New York: Dover Publications. 1995 reprint). San Francisco, California: W.H. Freeman and Co. 1964.

Leopold, L.B., W.W. Emmett, and R.M. Myrick. "Channel and Hillslope Processes in a Semiarid Area, New Mexico." U.S. Geological Survey Professional Paper 352-G. pp. 193–253. 1966.

Luhr, J. and T. Simkin. "Parícutin: The Volcano Born in a Mexican Cornfield." Phoenix, Arizona: Geoscience Press/Smithsonian Institution. 1993.

Major, J.J. "Post-Eruption Suspended Sediment Transport at Mount St. Helens: Decadal-Scale Relationships with Landscape Adjustments and River Discharges." *Journal of Geophysical Research*. Vol. 109. F01002, doi:10.1029/2002JF000010. 2004.

Major, J.J., T.C. Pierson, R.L. Dinehart, and J.E. Costa. "Sediment Yield Following Severe Volcanic Disturbance—A Two-Decade Perspective from Mount St. Helens." *Geology*. Vol. 28. No. 9. pp. 819–822. 2000.

Mayer, L. "Dating Quaternary Fault Scarps Formed in Alluvium Using Morphologic Parameters." *Quaternary Research*. Vol. 22. pp. 300–313. 1984.

Mohanty, S., R. Benke, R. Codell, K. Compton, D. Esh, D. Gute, L. Howard, T. McCartin, O. Pensado, M. Smith, G. Adams, T. Ahn, P. Bertetti, L. Browning, G. Cragnolino, D. Dunn, R. Fedors, B. Hill, D. Hooper, P. LaPlante, B. Leslie, R. Nes, G. Ofoegbu, R. Pabalan, R. Rice, J. Rubenstone, J. Trapp, B. Winfrey, and L. Yang. "Risk Analysis for Risk Insight Progress Report." San Antonio, Texas: CNWRA. 2005.

Mohanty, S., R. Codell, J.M. Menchaca, R. Janetzke, M. Smith, P. LaPlante, M. Rahimi, and A. Lozano. "System-Level Performance Assessment of the Proposed Repository at Yucca Mountain Using the TPA Version 4.1 Code." CNWRA 2002-05. Rev. 2. San Antonio, Texas: CNWRA. 2004.

Mosiño-Alemán, P.A. and E. García. "The Climate of Mexico." *Climates of North America*. R.A. Bryson and F.K. Hare (eds). Amsterdam: Elsevier. pp. 345–404. 1974.

Nash, D.B. "Forms of Bluffs Degraded for Different Lengths of Time in Emmet County, Michigan, USA." *Earth Surface Processes*. Vol. 5. pp. 331–345. 1980a.

———. "Morphologic Dating of Degraded Normal Fault Scarps." *Journal of Geology*. Vol. 88. pp. 353–360. 1980b.

———. "Morphologic Dating of Fluvial Terrace Scarps and Fault Scarps Near West Yellowstone, Montana." *Geological Society of America Bulletin*. Vol. 95. pp. 1413–1424. 1984.

National Oceanic and Atmospheric Administration. “Upper Air Data: Desert Rock, Nevada, 1978–1995.” Reno, Nevada: National Oceanic and Atmospheric Administration, Western Regional Climate Center. n.d. <http://www1.ncdc.noaa.gov/pub/data/ua>

NRC. “Risk Insights Baseline Report.” ML0405601620. Washington, DC: NRC. April 2004. <www.nrc.gov/waste/hlw-disposal/reg-initiatives/resolve-key-tech-issues.html>

———. “Issue Resolution Status Report, Key Technical Issue: Igneous Activity.” Rev. 2. Washington, DC: NRC, Division of Waste Management. 1999.

Pabst, M.E., D.A. Beck, P.A. Glancy, and J.A. Johnson. “Streamflow and Selected Precipitation Data for Yucca Mountain and Vicinity, Nye County, Nevada, Water Years 1983–85. U.S. Geological Survey Open-File Report 93–438. p. 66. 1993.

Peterson, F.F., J.W. Bell, R.I. Dorn, A.R. Ramelli, and T. Ku. “Late Quaternary Geomorphology and Soils in Crater Flat, Yucca Mountain Area, Southern Nevada.” *Geological Society of America Bulletin*. Vol. 107. pp. 379–395. 1995.

Pierce, K.L. and S.M. Colman. “Effect of Height and Orientation (Microclimate) on Geomorphic Degradation Rates and Processes, Late-Glacial Terrace Scarps in Central Idaho.” *Geological Society of America Bulletin*. Vol. 97. pp. 869–885. 1986.

Powell, D.M., I. Reid, J.B. Laronne, and L. Frostick. “Bed Load as a Component of Sediment Yield from a Semiarid Watershed of the Northern Negev.” Erosion and Sediment Yield: Global and Regional Perspectives (Proceedings of the Exeter Symposium, July 1996). IAHS Publication No. 236. pp. 389–397. 1996.

Reid, I., J.B. Laronne, and D.M. Powell. “The Nahal Yatir Bedload Database: Sediment Dynamics in a Gravel-Bed Ephemeral Stream.” *Earth Surface Processes and Landforms*. Vol. 20. pp. 845–857. 1995.

———. “Flash-Flood and Bedload Dynamics of Desert Gravel-Bed Streams.” *Hydrological Processes*. Vol. 12. pp. 543–557. 1998.

Renard, K.G. “Sediment Problems in the Arid and Semiarid Southwest.” Soil Conservation Society of America. The Earth Around Us: Proceedings of the 27th Annual Meeting. pp. 225–232. 1972.

Renard, K.G. and E.M. Laursen. “Dynamic Behavior Model of Ephemeral Stream.” *Journal of the Hydraulics Division*. American Society of Civil Engineering. Vol. 101. No. HY5. pp. 511–528. 1975.

Richtmyer, R.D. and K.W. Morton. “Difference Methods for Initial-Value Problems.” (2nd ed.). Interscience Publishers. New York City, New York: John Wiley & Sons. p. 405. 1967.

Ritter, D.F., R.C. Kochel, and J.R. Miller. “Process Geomorphology–4th ed.” New York City, New York: McGraw-Hill. 2002.

Savard, C.S. “Selected Hydrologic Data from Fortymile Wash in the Yucca Mountain Area, Nevada, Water Year 1992.” U.S. Geological Survey Open-File Report 94–317. p. 38. 1995.

———. “Selected Hydrologic Data from Fortymile Wash in the Yucca Mountain Area, Nevada, Water Years 1993–94.” U.S. Geological Survey Open-File Report 95–709. p. 30. 1996.

———. “Estimated Ground-Water Recharge From Streamflow in Fortymile Wash Near Yucca Mountain, Nevada.” U.S. Geological Survey Water-Resources Investigations Report 97–4273. p. 30. 1998.

Schick, A.P. and J. Lekach. “An Evaluation of Two Ten-year Sediment Budgets, Nahal Yael, Israel.” *Physical Geography*. Vol. 14. pp. 225–238. 1993.

Segerstrom, K. “Erosion Studies at Parícutin, State of Michoacán, Mexico.” U.S. Geological Survey Bulletin 965–A. p. 164. 1950.

———. “Erosion and Related Phenomena at Parícutin in 1957.” U.S. Geological Survey Bulletin 1104–A. pp. 1–18. 1960.

———. “Deceleration of Erosion at Parícutin, Mexico.” U.S. Geological Survey Professional Paper 424–D. pp. D225–D227. 1961.

———. “Parícutin, 1965—Aftermath of Eruption.” U.S. Geological Survey Professional Paper 550–C. pp. C93–C101. 1966.

Selby, M.J. “Hillslope Materials and Processes.” 2nd Edition. Oxford: Oxford University Press. 1993.

Sellers, W.D. and R.H. Hill (eds.). “Arizona Climate.” Tucson, Arizona: The University of Arizona Press. p. 616. 1974.

Simkin, T. and L. Siebert. “Volcanoes of the World.” 2nd ed. Tucson, Arizona: Geoscience Press. p. 349. 1994.

Smiley, T.L. “The Geology and Dating of Sunset Crater, Flagstaff, Arizona.” Ninth Field Conference, New Mexico Geological Society, Field Conference Guidebook. pp. 186–190. 1958.

Squires, R.R. and R.L. Young. “Flood Potential of Fortymile Wash and its Principal Southwestern Tributaries, Nevada Test Site, Southern Nevada.” U.S. Geological Survey Water-Resources Investigations Report 83–4001. p. 33. 1984.

Swanson, F.J., R.J. Janda, T. Dunne, and D.N. Swanston, tech. eds. “Sediment Budgets and Routing in Forested Drainage Basins.” General Technical Report PNW–141. Portland, Oregon: U.S. Department of Agriculture, Forest Service, Pacific Northwest Forest, and Range Experiment Station. p. 165. 1982.

Tanaka, K.L., T.C. Onstott, and E.M. Shoemaker. “Magnetostratigraphy of the San Francisco Volcanic Field, Arizona.” U.S. Geological Survey Bulletin 1929. p. 35. 1990.

Tanko, D.J. and P.A. Glancy. "Flooding in the Amargosa River Drainage Basin, February 23–24, 1998, Southern Nevada and Eastern California, Including the Nevada Test Site." U.S. Geological Fact Sheet 036–01. p. 4. 2001.

Thomas, B.E., H.W. Hjalmarson, and S.D. Waltemeyer. "Methods for Estimating Magnitude and Frequency of Floods in the Southwestern United States." U.S. Geological Survey Water-Supply Paper 2433. p. 195. 1997.

Tooth, S. "Process, Form and Change in Dryland Rivers: A Review of Recent Research." *Earth-Science Reviews*. Vol. 51. pp. 67–107. 2000.

Trimble, S.W. "A Sediment Budget for Coon Creek Basin in the Driftless Area, Wisconsin, 1853–1977." *American Journal of Science*. Vol. 283. pp. 454–474. 1983.

Waddell, R.K., J.H. Robison, and R.K. Blankennagel. "Hydrology of Yucca Mountain and Vicinity, Nevada-California—Investigative Results Through Mid–1983." U.S. Geological Survey Water-Resources Investigations Report 84–4267. p. 72. 1984.

Waldron, H.H. "Debris Flow and Erosion Control Problems Caused by the Ash Eruptions of Irazú Volcano, Costa Rica." U.S. Geological Survey Bulletin 1241–I. p. 37. 1967.

Walker, G.P.L. "Explosive Volcanic Eruptions–A New Classification Scheme." *Geologische Rundschau*. Vol. 62. pp. 431–446. 1973.

Walling, D.E. and A.H.A. Kleo. "Sediment Yields of Rivers in Areas of Low Precipitation: A Global View." The Hydrology of Areas of Low Precipitation (Proceedings of the Canberra Symposium, December 1979). IAHS–AISH Publication No. 128. pp. 479–493. 1979.

Whitney, J.W. and C.D. Harrington. "Relict Colluvial Boulder Deposits as Paleoclimatic Indicators in the Yucca Mountain Region, Southern Nevada." *Geological Society of America Bulletin*. Vol. 105. pp. 1,008–1,018. 1993.